Chem Soc Rev

REVIEW ARTICLE

Oligo(phenylenevinylene) hybrids and self-assemblies: versatile materials for excitation energy transfer

Cite this: DOI: 10.1039/c3cs60406c

Vakayil K. Praveen,*[a] Choorikkat Ranjith,[b] Elisa Bandini,[a] Ayyappanpillai Ajayaghosh*[c] and Nicola Armaroli*[a]

Oligo(phenylenevinylene)s (OPVs) are extensively investigated π-conjugated molecules that exhibit absorption and fluorescence in the UV-Vis spectral region, and which can be widely tuned by chemical functionalisation and external control (*e.g.* solvent, temperature, pH). Further modulation of the optoelectronic properties of OPVs is possible by supramolecular aggregation, primarily driven by hydrogen bonding or π-stacking interactions. In recent years, extensive research work has been accomplished in exploiting the unique combination of the structural and electronic properties of OPVs, most of which has been targeted at the preparation of molecules and materials featuring photoinduced energy transfer. This review intends to offer an overview of the multicomponent arrays and self-assembled materials based on OPV which have been designed to undergo energy transfer by means of a thorough choice of excitation donor–acceptor partners. We present a few selected examples of photoactive dyads and triads containing organic moieties (*e.g.* fullerene, phenanthroline) as well as co-ordination compounds (Cu(I) complexes). We then focus more extensively on self-assembled materials containing suitably functionalised OPVs that lead to hydrogen bonded aggregates, helical structures, gels, nanoparticles, vesicles, mesostructured organic–inorganic hybrid films, functionalised nanoparticles and quantum dots. In most cases, these materials exhibit luminescence whose colour and intensity is related to the efficiency and direction of the energy transfer processes.

Received 9th November 2013

DOI: 10.1039/c3cs60406c

www.rsc.org/csr

1. Introduction

Light absorption followed by excitation energy transfer within or between molecular units is a key process in both biological and synthetic systems.[1–11] Such a process requires the strictest control of the direction and efficiency of the energy transduction in order to guarantee a reliable high-quality output, typically light emission or excitation harvesting at a given point. Such a complex goal can be achieved by integrating energy transfer donor–acceptor systems in a single molecular structure or by self-assembling them through highly selective and directional supramolecular interactions such as hydrogen bonding or π-stacking interactions.[1–11] In this context, π-conjugated molecules with different optical band gaps have been widely used as donor and/or acceptor molecules. Among a plethora of π-conjugated systems synthesized in the last two decades,[12,13] oligo(phenylenevinylene)s (OPVs) have received enormous attention, mainly due to their well-defined molecular structure and tunable optical properties in the UV-Vis spectral region. A key approach towards the modulation of the optoelectronic properties of OPVs is that based on self-assembly, which takes advantage of the peculiar properties of OPVs that are very sensitive to intermolecular interactions and molecular organisation.[14–17] Indeed, excitation energy transfer from OPVs to various acceptors have sparked wide interest, owing to possible applications in molecular and supramolecular electronics.[18,19]

Through the illustration of selected examples, we provide herein an overview and perspective on photoactive multicomponent systems and self-assembled materials containing OPVs, which have been designed to feature excitation energy transfer. The main target of this research is to obtain luminescent materials exhibiting any emission colour in the visible as well as near infrared (NIR) region, including white. This is made possible by the combination of several strategies: the thorough choice of donor–acceptor partners even in combination with ancillary components providing peculiar extra properties, establishment of selective supramolecular interactions, engineering of the direction and extent of the energy transfer. This concerted

---

[a] *Istituto per la Sintesi Organica e la Fotoreattività, Consiglio Nazionale delle Ricerche (ISOF-CNR), Via Gobetti 101, 40129 Bologna, Italy. E-mail: praveen.karthikeyan@isof.cnr.it, nicola.armaroli@isof.cnr.it; Web: http://www.isof.cnr.it/?q=content/armaroli-nicola*

[b] *Dipartimento di Chimica Organica, Università degli Studi di Milano, Via Golgi 19, 20133 Milano, Italy*

[c] *Photosciences and Photonics Group, Chemical Sciences and Technology Division, CSIR-National Institute for Interdisciplinary Science and Technology (CSIR-NIIST), Trivandrum 695019, India. E-mail: ajayaghosh@niist.res.in; Web: http://www.niist.res.in/english/scientists/ajayaghosh-a-/personal.html*

effort may provide luminescent materials with exceptional structural and morphological properties both as gels and solids, which may open up wide possibilities for exploitation in the area of organic electronics and smart materials.[18,19]

2. Non radiative excitation energy transfer

The non-radiative transfer of electronic energy from an initially excited donor molecule (D) to an acceptor (A) in the ground state is a phenomenon of great fundamental and practical importance.[20–22] The key requirements for such a process are: (i) the energy of the donor excited state must be higher than that of the acceptor excited state and (ii) the rate of energy transfer must be faster than the intrinsic decay rate of the excited donor. Electronic energy transfer, which typically occurs upon photoexcitation of an energy donor by UV-Vis light, can take place either by electron exchange between D and A (Dexter mechanism) or through a coulombic dipole–dipole interaction (Förster mechanism).[20] The former needs an overlap of the wavefunctions between the two partners in order to allow the electron exchange, hence it may take place over short distances, typically within 10 Å; in the latter one the interaction occurs through space *via* electromagnetic interactions and can therefore occur over longer D–A distances. The Dexter mechanism can be described schematically as depicted in Fig. 1a, with two electron exchange processes

Vakayil K. Praveen

Vakayil K. Praveen completed his PhD at University of Kerala (2007) under the guidance of A. Ajayaghosh (NIIST, India). He then worked as a postdoctoral fellow in the research group of Takuzo Aida, University of Tokyo, Japan, funded by the GCOE (2007) and JSPS (2009) programmes. In 2011, he moved to Istituto per la Sintesi Organica e la Fotoreattività (CNR-ISOF), Italy, after qualifying for a European Commission Marie Curie International Incoming Fellowship (FP7), conducting his research under the supervision of Nicola Armaroli. His research interests are the synthesis, self-assembly and photophysical properties of π-conjugated molecules and their hybrids.

Choorikkat Ranjith

Ranjith Choorikkat obtained his PhD from the University of Calicut, Kerala (India) in 2008 with K. K. Vijayan. His research was focused on the synthesis and characterization of photoactive heterocyclic compounds with biological properties. He then worked in leading chemical companies (GE Global Research, Syngenta Biosciences Pvt. Ltd and Porus Laboratories Pvt. Ltd) as a research scientist. Presently he is a postdoctoral researcher at the Università degli Studi di Milano, Italy, in a project funded by ENI on organic molecules for DSSCs and polymer solar cells, in the group of Emanuela Licandro. His research interests are focussed on synthetic organic chemistry and photochemistry.

Elisa Bandini

Elisa Bandini joined the Italian National Research Council (CNR) as technical research assistant in 1986. She obtained her PhD at the University of Bologna in 2006, under the guidance of Mauro Panunzio. She participated in the Executive Protocol of S&T cooperation between China and Italy during 2006–2009. She has worked in several research projects funded by leading industries (Lek-Novartis, Polarchemie, Nicox). In 2012, she was promoted to staff researcher at CNR-ISOF, Bologna. Her research interests include the stereoselective synthesis of biologically active molecules, microwave chemistry and the design and synthesis of photo- and electroactive functional molecules.

Ayyappanpillai Ajayaghosh

Ayyappanpillai Ajayaghosh is a CSIR Outstanding Scientist at the NIIST Trivandrum, and Professor and Dean of Chemical Sciences, Academy of Scientific and Innovative Research , New Delhi, India. He has received several awards including the Shanti Swarup Bhatnagar Prize, Thomson Reuters Research Excellence-India Research Front Award and the Infosys Prize. He is a fellow of all three science academies of India. His research interests include supramolecular and macromolecular chemistry, organogels, functional dyes and fluorophores, photoresponsive materials, molecular probes for sensing and imaging. He is an associate editor of Physical Chemistry Chemical Physics and a board member of Chemistry–An Asian Journal and RSC Advances.

This journal is © The Royal Society of Chemistry 2014

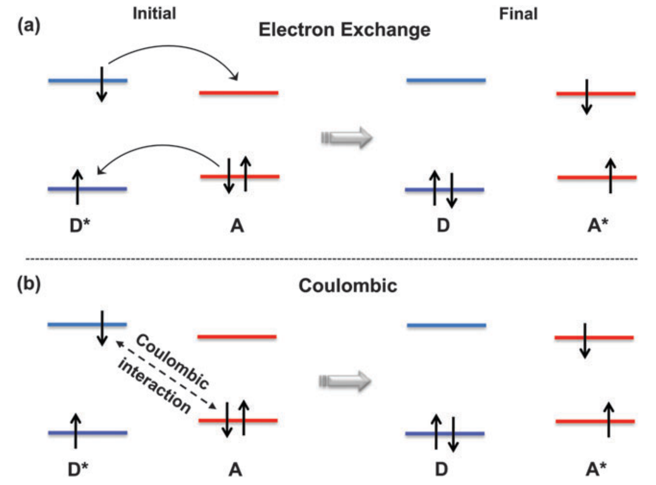

Fig. 1 Schematic representation of non-radiative energy transfer processes. (a) Dexter electron exchange mechanism and (b) Förster coulombic mechanism. 'D' is the energy donor, 'A' is the energy acceptor and * denotes an excited state.

occurring simultaneously.[20] One involves the transfer of the excited electron of D to the lowest unoccupied molecular orbital (LUMO) of A, the other one occurs between the highest occupied molecular orbital (HOMO) of A to the corresponding orbital of D. The exchange interaction requires that D and A are close enough to allow the overlapping of the orbitals involved and the rate of this process decreases exponentially with distance (eqn (1)),

$$k_{\mathrm{ET}} = KJ\,\exp(-2d/L) \tag{1}$$

where K is related to the specific orbital interactions, d is the donor–acceptor separation, L is the sum of the van der Waals radii, and J is the normalized spectral overlap integral, which is related to the degree of overlap between the emission spectrum of the donor and the absorption spectrum of the acceptor (eqn (2)),

$$J = \int_0^{\infty} F_{\mathrm{D}}(\bar{\nu})\varepsilon_{\mathrm{A}}(\bar{\nu})\mathrm{d}\bar{\nu} \tag{2}$$

where $F_{\mathrm{D}}(\bar{\nu})$ is the corrected luminescence spectrum of the donor and $\varepsilon_{\mathrm{A}}(\bar{\nu})$ is the absorption spectrum of the acceptor, each normalized to unity and on a wavenumber scale.

The Förster mechanism can be represented as a through-space interaction, where the excited D unit (D*) and its related A partner ''feel'' each other's presence *via* long range coulombic forces. The basic mechanism involves the interaction of the D* dipole (*i.e.* the excited electron in the LUMO) with the A dipole (*i.e.* an unexcited electron in the HOMO) that ultimately leads to the process schematicized in Fig. 1b.[20] The rate of energy transfer in this case is given by eqn (3):

$$k_{\mathrm{ET}} = \frac{1}{\tau_{\mathrm{D}}}\left(\frac{R_{\mathrm{c}}}{d}\right)^{6} \tag{3}$$

where τ_{D} is the excited state lifetime of D in the absence A, and d is the donor–acceptor distance. R_{c} is the so called critical radius, namely the distance at which the energy transfer rate k_{ET} is equal to the intrinsic decay rate of the donor and is described by eqn (4). R_{c} is typically in the range of 20 to 60 Å and it can be as large as 100 Å for efficient acceptors; it is described by eqn (4):

$$R_{\mathrm{c}}{}^{6} = \frac{9000(\ln 10)K^{2}\Phi_{\mathrm{D}}}{128\pi^{5}Nn^{4}}J \tag{4}$$

where K^2 is the orientation factor (related to the relative orientation of the donor and acceptor dipoles),[20] Φ_{D} is the emission quantum yield of D in the absence of A, n is the refractive index of the solvent, N is the Avogadro's number and J is the spectral overlap integral (eqn (2)). As derived from eqn (3), the rate of energy transfer according to the Förster mechanism is inversely proportional to the sixth power of the D–A separation, which is a substantial difference with respect to the Dexter mechanism.[20]

The efficiency of energy transfer depends upon the distance and relative orientation between the donor–acceptor chromophores. In natural light harvesting assemblies, these crucial parameters are satisfied by organizing key pigment molecules in a fixed spatial relationship by the surrounding medium with the help of non-covalent interactions, which ultimately results in an efficient and directional energy transfer processes.[21,22]

Energy transfer mechanisms strongly depend on the spin of the initial and final species.[20] In the case of OPV chromophores, the lowest excited state is a singlet and typically sensitises a singlet level of the acceptor. Such ''singlet–singlet'' energy transfer is permitted for both Förster and Dexter mechanisms,[20] which renders OPVs excellent energy transfer donors in the presence of suitably selected singlet acceptors, as extensively described herein.

Nicola Armaroli

Nicola Armaroli obtained his PhD in 1994. After post-doctoral work in the U. S. and Italy, in 1997 he joined the Italian National Research Council, becoming Research Director in 2007. His activity is concerned with the photochemistry/photophysics of molecular and supramolecular materials targeted at lighting technologies and solar energy conversion. He has published over 180 papers and 5 books and is a lecturer and consultant on issues of energy and natural resources. He is a member of the Editorial Board of Chemistry–A European Journal, an associate editor of Photochemical & Photobiological Sciences (RSC) and chairman of the Working Party on Chemistry and Energy of EuCheMS.

3. OPVs as excitation energy donors

OPVs are known to be efficient excitation energy donors and several dyads, in which they are coupled with suitable acceptors, have been reported in the literature. Among them, OPV–fullerene (C_{60}) systems have been extensively studied[23,24] due to their possible application in photovoltaic devices.[25,26] A characteristic feature of all of these dyads is an ultrafast singlet–singlet energy transfer from the OPV unit (placed at around 3 eV, in the case of OPV trimers) to populate the lowest singlet state of fullerene ($\approx$1.7 eV).[27] Once the latter electronic state is populated, an OPV → fullerene electron transfer may occur, provided that the polarity of the solvent is sufficiently high (*e.g.* in benzonitrile).[28–30] A more sophisticated example of a photoactive OPV–fullerene system is **1** (Fig. 2). In this case, C_{60} is equipped with both an energy (OPV) and an electron donor (pyrazoline) unit. Selective UV excitation of the OPV unit promotes an OPV → fullerene energy transfer, whereas excitation of the carbon sphere in the visible spectral region triggers a pyrazoline → fullerene electron transfer. The latter process can be switched on/off by protonation/deprotonation of the pyrazoline nitrogen, temperature increase/decrease, and solvent polarity.[28,30]

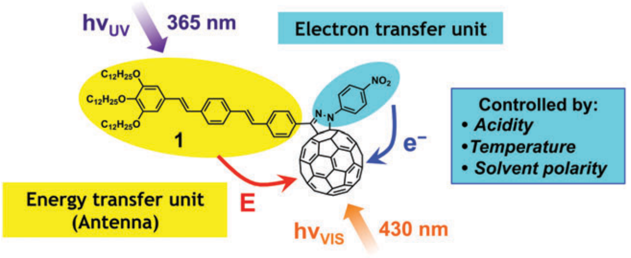

Fig. 2 OPV–C_{60}–pyrazoline triad (**1**) where the fullerene unit acts as the energy or electron acceptor for the OPV and the pyrazoline moiety, respectively. (Adapted with permission from ref. 30. Copyright 2003 European Society for Photobiology, the European Photochemistry Association, and The Royal Society of Chemistry.)

Though the energy transfer process in various molecular dyads has been studied extensively, a more challenging task is the control of the *direction* of energy transfer in such a type of system. This was achieved with an OPV–phenanthroline molecular dyad that was designed to function as a proton-triggered molecular switch (Fig. 3).[31,32] The electronic level of OPV is intermediate in energy relative to that of phenanthroline (Phen) and protonated phenanthroline, (Phen$^{\bullet}$H^{+}). Thus, in the OPV–Phen dyad **2a**, upon selective light excitation of the phenanthroline unit, a Phen → OPV photoinduced energy transfer occurs; on the other hand, upon acidification of the solution, **2a** is converted into **2b**, and OPV becomes the energy donor for the Phen$^{\bullet}$H^{+} unit. Therefore, the direction of energy transfer is controlled by means of the reversible protonation/deprotonation of the phenanthroline unit, which is signalled by the on/off switching of the intense blue fluorescence of the OPV moiety.

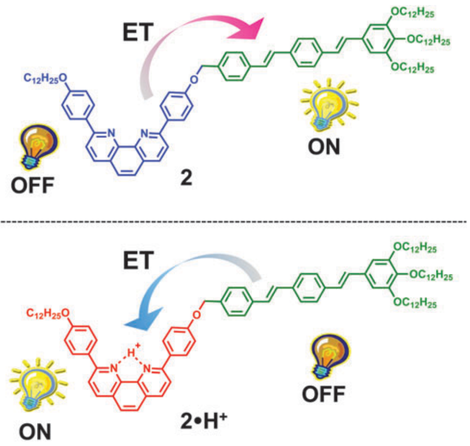

Fig. 3 Schematic representations showing the functioning of an OPV–phenanthroline molecular switch. (Adapted with permission from ref. 32. Copyright 2009 The Royal Society of Chemistry.)

The energy transfer from OPVs to doped or covalently linked organic dyes has been investigated in detail with the aim of tuning the optical and electronic properties of light emitting devices (LEDs) or photovoltaic systems.[33–41] For example, a poly(propylene imine) dendrimer functionalised with OPVs (**3**) was reported to transfer excitation energy to different encapsulated organic dyes (Fig. 4).[33] Owing to its amphiphilic nature, the OPV functionalised dendrimer served as a host capable of extracting water-soluble organic dyes (sulforhodamine B, rhodamine B, rhodamine 6G, and sulforhodamine 101) into the organic phase. The resulting host–guest system facilitates energy transfer from the peripheral OPV units to the encapsulated dye molecules with 40% efficiency.

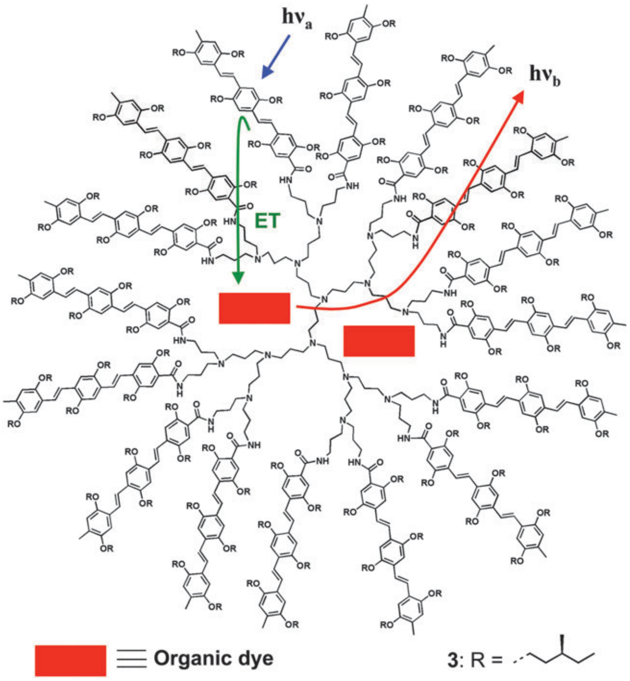

Fig. 4 A schematic representation of the energy transfer process in an amphiphilic OPV dendrimer (**3**) encapsulated with a water-soluble organic dye (sulforhodamine B, rhodamine B, rhodamine 6G, and sulforhodamine 101). (Adapted with permission from ref. 33. Copyright 2000 American Chemical Society.)

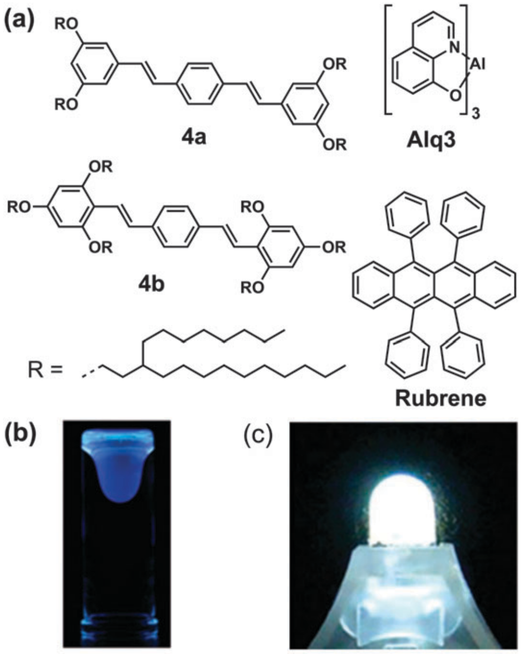

Fig. 5 (a) Molecular structures of OPVs and energy transfer acceptors Alq3 and rubrene. (b) Image of **4a** under UV light (365 nm). (c) Image of commercially available UV-LED (375 nm) after coating with white light emitting liquid composite. (Adapted with permission from ref. 40. Copyright 2012 Wiley-VCH.)

Notably, these systems also show excellent film forming properties without phase separation of the encapsulated organic dyes. Enhanced efficiency in energy transfer from the OPV (90%) is observed, which is attributed to a more favourable orientation and improved spectral overlap between the donor and acceptor molecules in the thin films.

Nakanishi and co-workers recently reported an interesting work on liquids that emit white-light at room temperature and are based on blue OPV luminophores (Fig. 5).[40] OPV derivatives are equipped with branched aliphatic hydrocarbons that perturb the intermolecular π–π interactions of the OPV core by steric hindrance and behave as low-viscosity room temperature liquids. The inhibition of the π–π interactions between OPV chromophores is evidenced through absorption and emission studies. The white-light emitting composites were prepared by mixing **4a** or **4b** with green emitting tris(8-hydroxyquinolinato)aluminium (Alq3) and orange-emitting rubrene in the molar ratio of 1 : 1.65 : 0.23. The reduced interface resistance between the components apparently facilitates partial energy transfer between the matrix host and the guest molecules, affording white-light emission with chromaticity diagram coordinate values of 0.33, 0.34 (CIE – Commission Internationale de l'Eclairage, 1931). As a practical application, white-light emitting liquid composites were used as an ink to write on solid surfaces and as coating materials for UV LEDs (Fig. 5c).

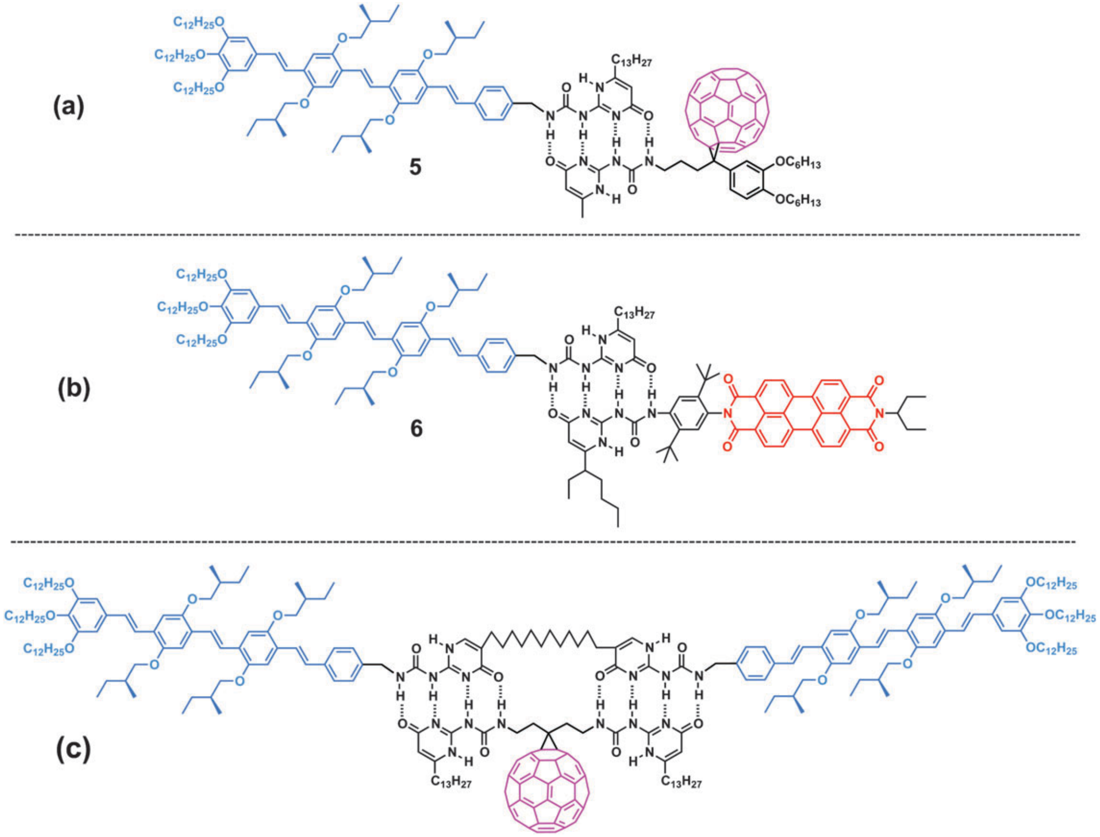

Fig. 6 OPV–C_{60} (**5** and **7**) and OPV–PBI (**6**) hydrogen bonded assemblies.

4. Energy transfer in hydrogen bonded assemblies of OPVs

Among the various noncovalent interactions, hydrogen bonding has emerged as a powerful tool to organise donor–acceptor chromophores undergoing photoinduced energy transfer.[42–44] Due to its tunable strength as a function of the residues involved (4–120 kJ mol^{-1}), directionality and specificity, hydrogen bonding enables highly versatile approaches for the preparation of supramolecular architectures.

Over the years, Meijer, Janssen and coworkers have extensively investigated energy transfer processes in hydrogen bonded OPV self-assemblies. An interesting case is the quadruple hydrogen bonded donor–acceptor dyad, **5** (Fig. 6a), which is constructed by attaching the self-complementary 2-ureido-4[1*H*]-pyrimidinone (UP) unit to an OPV donor and C_{60} acceptor.[45,46] Steady-state emission studies revealed that 90% quenching of the donor emission is due to singlet energy transfer to the C_{60} moiety; such a strong quenching is a consequence of the high association constant of the quadruple hydrogen bonded hetero-dimers. Later, the same approach was applied to a perylene bisimide energy acceptor (OPV–PBI, **6**, Fig. 6b).[47] In **5** and **6**, self-complementary hydrogen bonding leads to a statistical mixture of homo- and hetero-dimers. By contrast dyad **7** (Fig. 6c), in which one of the two components is equipped with two UP units, shows preferential formation of hetero-dimers as evidenced by ^{1}H NMR.[48] Photoluminescence studies of **7** show excitation energy transfer from the OPV to the C_{60} moiety. Electron transfer is thermodynamically allowed but does not occur due to the weak electronic coupling between the donor and the acceptor, as a result of the long interchromophoric distance.[48]

Schenning, Meijer and co-workers have demonstrated energy transfer in hydrogen bonded helical co-assemblies of OPVs **8a** and **8b**, which are characterized by different conjugation lengths and bear an identical ureido-*s*-triazine (UT) hydrogen bonding motif (Fig. 7).[49–51] Fast and efficient energy transfer from shorter to longer oligomers is observed by increasing the concentration of the acceptor molecules, as monitored by the decrease in photoluminescence (PL) intensity of the donor (Fig. 7b). Up to about a concentration of 2% with respect to the donor, the acceptor molecules exist only as isolated energy traps. At higher concentrations they undergo clustering, as evidenced by a decrease in the characteristic fluorescence band in diluted solution, accompanied by the onset of a red-shifted feature typical of aggregates.

A theoretical study by Jang *et al.*, suggests that the rate of energy transfer in multi-chromophoric systems can be controlled by chromophore arrangement.[52] This has been experimentally proved by Schenning, Meijer and co-workers using ordered and disordered assemblies of OPVs.[53–55] When compared to the well ordered assembly of **8a**, the dimeric analogue **9** forms disordered polymeric aggregates due to the presence of a spacer between the hydrogen bonding units (Fig. 8). Fluorescence titration studies with **8c** as an energy acceptor show that the quenching efficiency at similar amounts of acceptor is

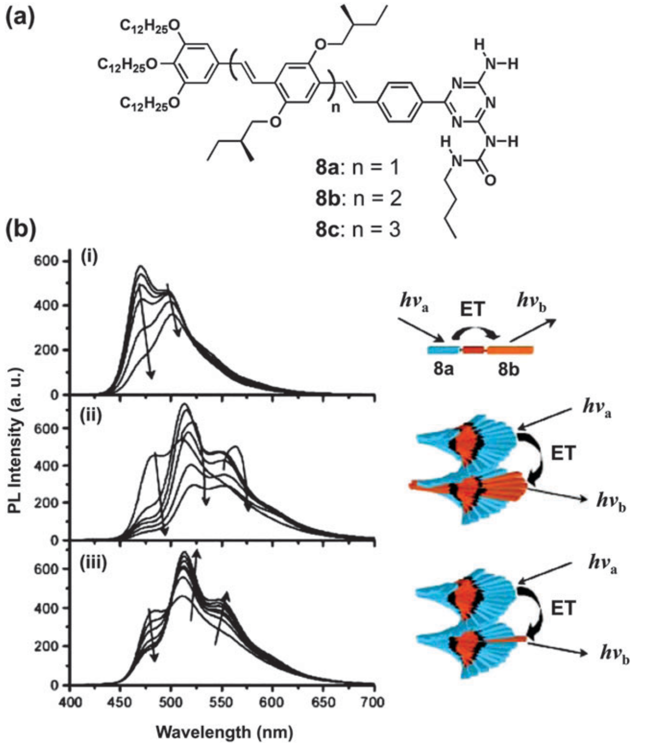

Fig. 7 (a) Molecular structures of ureido-*s*-triazine functionalised OPVs. (b) Photoluminescence spectra for mixtures of **8a** and **8b** in *n*-dodecane solution (λ_{ex} = 412 nm). The concentration of **8a** is fixed at 1.9 × 10^{-5} M: (i) 0–30 mol% **8b** at 80 °C (ii) 0–30 mol% **8b** at 10 °C (iii) 0–1.2 mol% **8b** at 10 °C. (Adapted with permission from ref. 49. Copyright 2004 Wiley-VCH.)

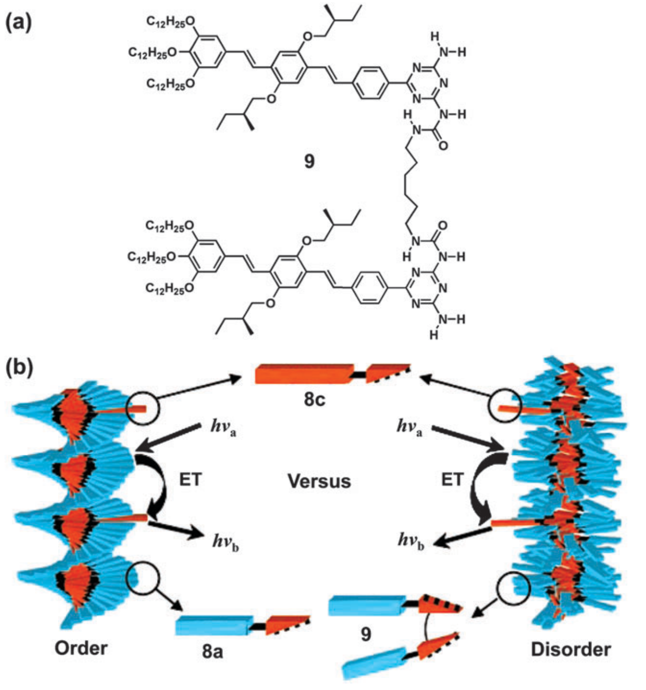

Fig. 8 (a) Molecular structure of bifunctional ureido-*s*-triazine functionalised OPV. (b) Schematic representation of the energy transfer processes in helically ordered and disordered assemblies of **8a** and **9**, respectively. (Adapted with permission from ref. 53. Copyright 2005 Wiley-VCH.)

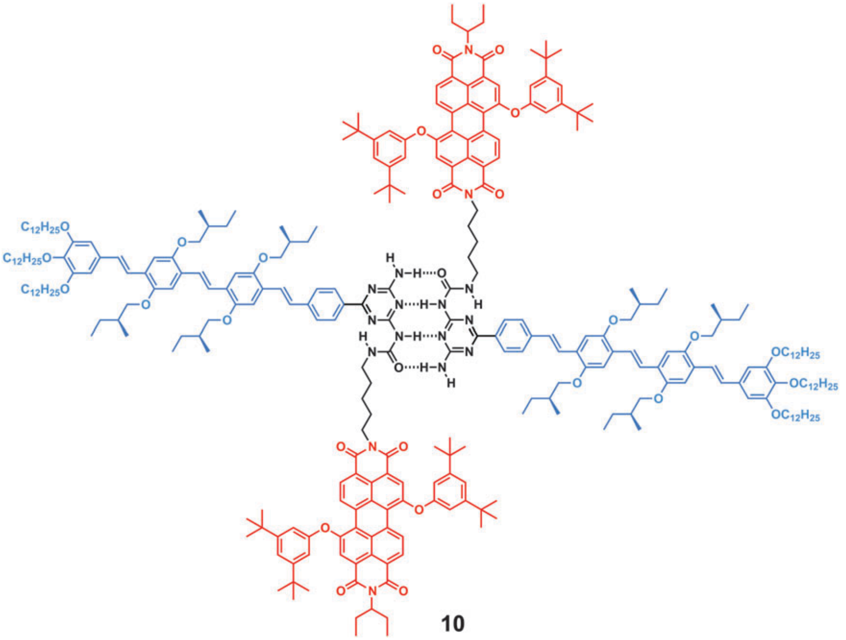

10

Fig. 9 Hydrogen bonded assembly of a OPV–PBI dyad functionalised with ureido-*s*-triazine.

significantly higher for the well-ordered stacks of **8a** when compared to those of the disordered aggregates of **9**.[53–55] Time-resolved fluorescence studies suggest that the ordered helical assembly of **8a** undergoes a fast initial fluorescence depolarization and excitation transfer to the dopant, which is in agreement with semi-coherent exciton diffusion along the chiral stacks of **8a**.[54] For the disordered polymeric assemblies of **9**, both depolarization and energy transfer dynamics take place on a much longer time scale, which is attributed to a weak electronic coupling of the chromophoric units that leads to slow incoherent motion of the excitations along the stacks of **9**.[54]

Energy transfer was also reported to occur in the ureido-*s*-triazine functionalised OPV–PBI dyad **10**, in which the PBI unit is covalently attached to the ureido unit of the OPV–UT moiety through a flexible linker (Fig. 9).[56] Photoluminescence studies of mixed assemblies formed by the OPV–PBI dyad (**10**) and OPV–UTs (**8a** or **8b**) in chloroform or *n*-dodecane show strong quenching of the OPV–UT emission with a concomitant rise in the PBI luminescence. This indicates the occurrence of energy transfer in the hetero-dimers formed by **10** with **8a** or **8b**. Moreover, in *n*-dodecane, incorporation of **10** into the columnar aggregates of pure OPV–UTs (**8a** or **8b**) results in more effective energy transfer from the OPVs to the PBI unit.

The strength and directionality of the triple hydrogen bonding array of melamine and cyanuric acid has been utilised for the self-assembly of OPV–porphyrin donor–acceptor systems.[57] The porphyrin unit was functionalised with the cyanuric acid motif affording two sites for hydrogen bonding with the OPVs, which in turn are equipped with *s*-triazine units (OPV*n*Ts). Addition of the porphyrin derivative to OPV*n*Ts yields the hydrogen bonded complex **11** (Fig. 10) in which quenching of the OPV photoluminescence is observed due to aggregation as well as energy transfer. Detailed optical and chiro-optical studies provide ample evidence for the formation of chiral co-assemblies, which is facilitated by an additional π–π interaction provided by the porphyrin unit.

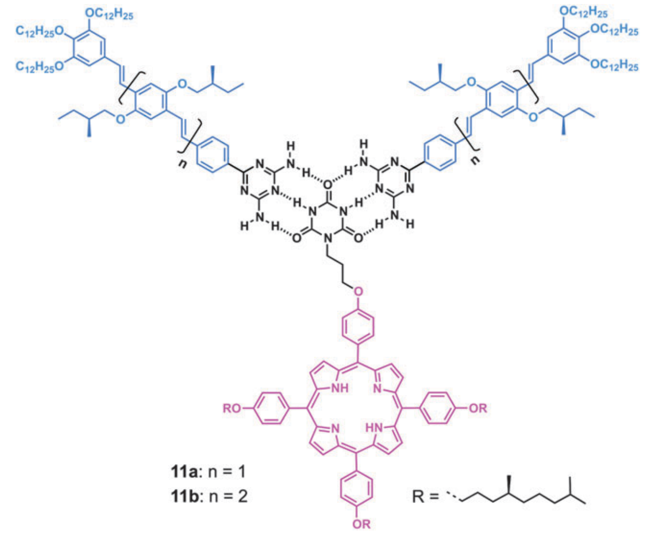

Fig. 10 Hydrogen bonded assembly of OPVs functionalised with *s*-triazine and a porphyrin equipped with cyanuric acid.

5. OPV-based light harvesting gels

Supramolecular gel formation is known to facilitate the alignment of donor–acceptor chromophores, thus favouring efficient light harvesting and energy transfer.[5,58–60] One of the most useful features obtained upon gelation of OPV derivatives is the tuning of their photophysical properties.[61–65]

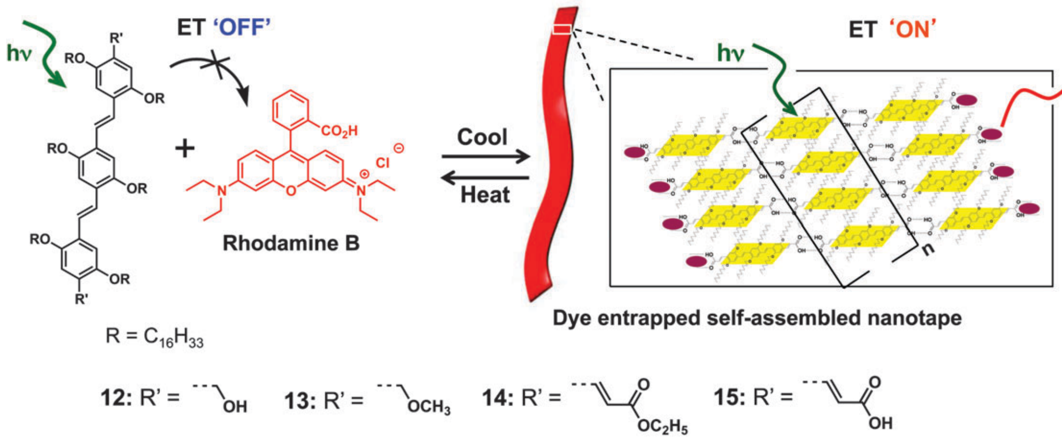

Fig. 11 Schematic representation of FRET from OPVs to rhodamine B within the self-assembled gel nanostructure (Adapted with permission from ref. 69. Copyright 2006 American Chemical Society.)

For instance, efficient exciton migration within aggregates of OPVs[65–67] may occur, prompting their use as excitation energy donors in combination with suitable acceptor molecules.

Excitation energy transfer from OPV gel nanostructures to an entrapped rhodamine B dye (Fig. 11) has been demonstrated by some of us.[68,69] Energy transfer is found to occur exclusively from the self-assembled OPVs and not from the individual molecule to the rhodamine B dye. Detailed studies show that the efficiency of energy transfer depends on the ability of the OPVs to form self-assemblies, which is strongly influenced by the structure of the gelator as well as the choice of the solvent. Moreover, the thermally reversible self-assembly of OPV derivatives enable control of the efficiency of energy transfer as a function of temperature. On the basis of photophysical and morphological studies, a plausible arrangement of the rhodamine dye entrapped in the OPV gel nanostructure was proposed (Fig. 11).

In another report, OPVs substituted with various end functional groups having tunable electron withdrawing characters have been utilised as excitation energy donors and acceptors.[64] The optical properties of the gel forming molecule **16a** (donor, Fig. 12) and the non-gelating molecule **17** (acceptor, Fig. 12) have been found to be optimal for carrying out energy transfer studies. Addition of **17** (2.6 mol%) to the *n*-decane gel of **16a** shows 90% quenching of the emission of the latter (Fig. 13a).

Control over the supramolecular assemblies of donors and acceptors in the nanoscale that facilitate efficient energy transfer and tunable emission has been demonstrated with **18** and **19** (Fig. 12).[70] Excitation of the donor gel **18** in *n*-decane at 380 nm in the presence of 2 mol% of **19** results in quenching of the emission band of the former ($\lambda_{\max}$ = 509 nm) with concomitant formation of the monomer and emission of the latter at 555 nm (Fig. 13b). Upon further addition of **19** (2–20 mol%), the emission is continuously red-shifted to 610 nm, which corresponds to the aggregate emission of this species (Fig. 13b). Fluorescence microscopy studies of the coassembled gels of **18** and **19** at different compositions provide visual evidence of the emission colour tuning by energy transfer (Fig. 13b). Thus, efficient trapping of excitons by acceptors as ''isolated'' or ''aggregated'' species allows a continuous shifting of the emission colour (Fig. 13c). In another report, the structure–property relationship of the energy transfer properties of

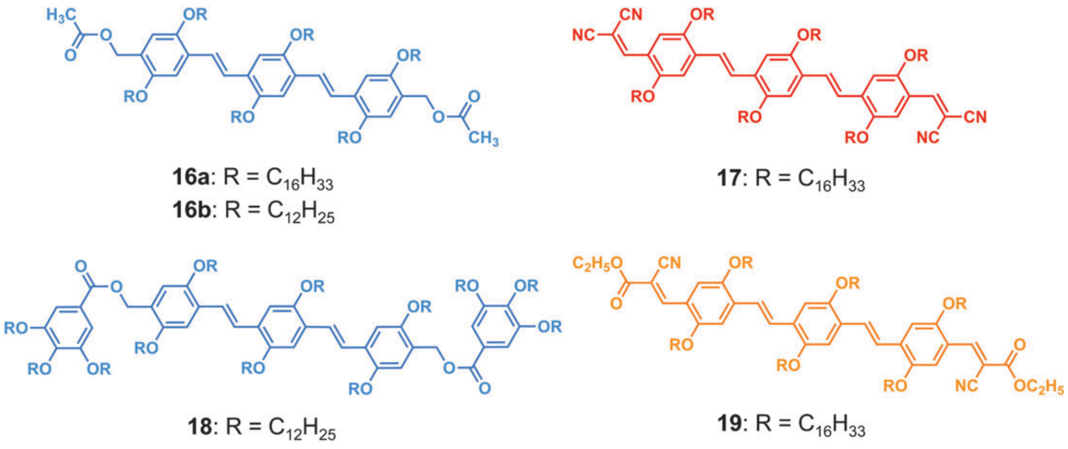

16a: R = $C_{16}H_{33}$
16b: R = $C_{12}H_{25}$

17: R = $C_{16}H_{33}$

18: R = $C_{12}H_{25}$

19: R = $C_{16}H_{33}$

Fig. 12 Molecular structures of OPV-based energy transfer donors (**16** and **18**) and acceptors (**17** and **19**).

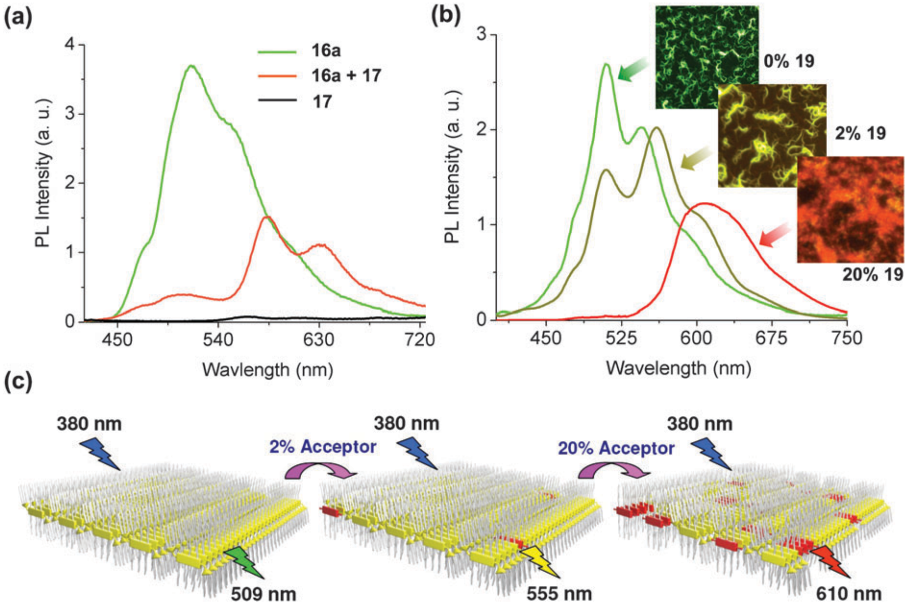

Fig. 13 (a) The energy transfer between **16a** and **17** (2.6 mol%) in an *n*-decane gel, λ_{ex} = 380 nm. (b) Emission spectra (λ_{ex} = 380 nm) and corresponding fluorescence microscopy images of **18** in the presence of 0.2 and 20 mol% of **19**. ((a) Adapted with permission from ref. 64. Copyright 2007 Wiley-VCH. (b and c) Adapted with permission from ref. 70. Copyright 2006 American Chemical Society.)

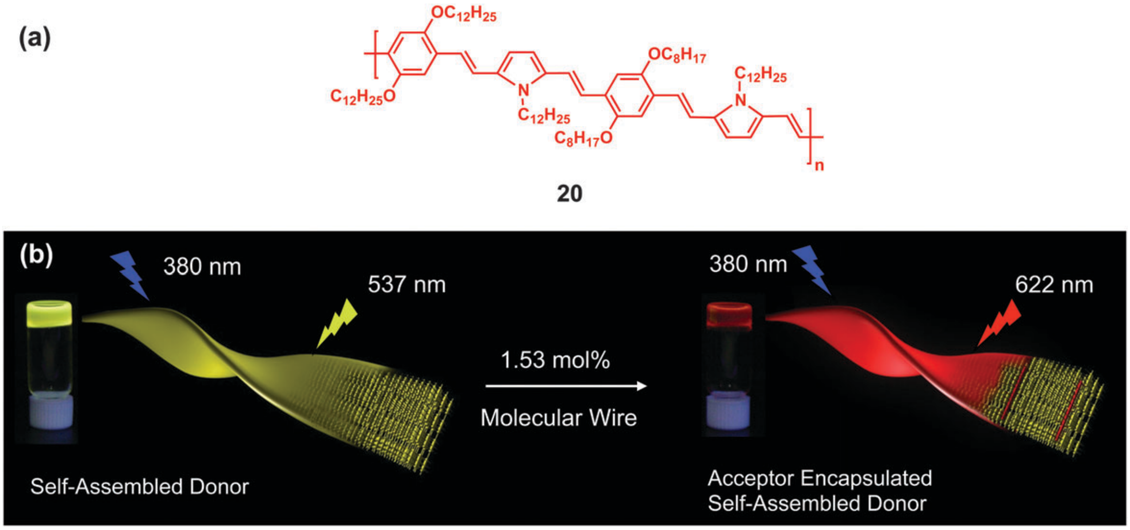

Fig. 14 (a) Molecular structure of the energy transfer acceptor phenylenevinylene-*co*-pyrrolylenevinylene oligomer (**20**). (b) A schematic representation of the energy transfer process between the gel forming OPV **12** and the molecular wire **20**. (Adapted with permission from ref. 65. Copyright 2007 Wiley-VCH.)

the OPV gelators were studied using steady-state and time-resolved fluorescence spectroscopy.[67] These studies show that the OPV donor **16b**, having small functional end groups (Fig. 12), exhibits better energy migration properties than **18**, which is equipped with bulkier terminal units. The energy transfer efficiency of **16b** is 82% whereas that of **18** is 42%, even at a low concentration of the acceptor **19** (3.1 mol%).

The use of the polymeric molecular wire **20**, for trapping the excitation energy of the OPV donor **12** (Fig. 11) led to the development of a light harvesting antenna within a supramolecular gel (Fig. 14).[65] Highly efficient energy migration was observed in the presence of a very small amount of the acceptor (<1.6 mol%). Time-resolved luminescence studies show a fast energy migration along the OPV donor scaffold (k_{EM} = 1.28 × 10^{10} s^{-1}), which ultimately facilitates the funnelling of the excitation energy to the encapsulated molecular wires.

Interestingly, the temperature dependent self-assembly of the donor gel **12** leads to a reversible change in energy transfer efficiency and emission colour (Fig. 15).[65,71] By increasing the temperature, the red-light emitting gel forms a blue-light emitting solution (70 °C) *via* the formation of an intermediate

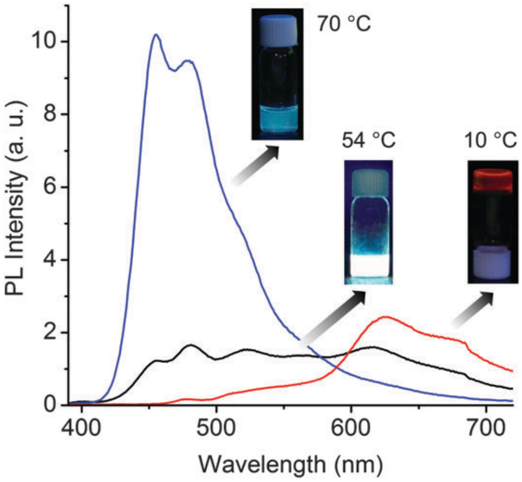

Fig. 15 Temperature dependence of the energy transfer between **12** (4×10^{-5} M) and **20** (1.53 mol%) in cyclohexane (λ_{ex} = 380 nm). The inset shows the corresponding emission colour under illumination at 365 nm. (Adapted with permission from ref. 65. Copyright 2007 Wiley-VCH.)

white-light emitting solution at 54 °C. The self-assembly partially dissociates into smaller aggregates and monomers at temperatures between 50 and 60 °C. White-light emission is generated by the combination of (i) blue luminescence of the monomers, (ii) residual green emission from the aggregates, and (iii) red emission from the acceptor upon partial energy transfer.[65,71]

The aforementioned report suggests that tunable emission colours can be achieved by controlling the self-organisation of the donor in combination with the energy transfer process to a suitable acceptor.[71] This has been further demonstrated by studies in organogels derived from cholesterol appended OPV derivatives (Fig. 16) in the presence of acceptor **20**.[66] The mono-cholesterol-OPV (**21**) forms a strong gel made of coiled helical tapes in which the chromophores are packed as pseudo J-type aggregates, whereas the bis-cholesterol-OPV (**22**) forms a weak gel through the hierarchical self-assembly of pseudo H-type aggregates leading to twisted helical tapes. This difference in molecular packing results in distinct photophysical behaviours, particularly excitation energy migration. In the case of **21**, strong gelation and fast exciton diffusion afford an efficient energy transfer (90%) to the encapsulated acceptor (2 mol%) with bright red emission typical of **20** (Fig. 15). On the other hand, weak gelation and slow energy migration bring about partial energy transfer (63%) from **22** to **20**, leading to white emission (Fig. 16).[66,71]

Samanta and Bhattacharya have reported light harvesting in mixtures of OPV-based gels (Fig. 17) made through the combination of intermolecular hydrogen bonding, π-stacking and van der Waals interactions.[72] A cascade of energy transfer processes is observed for chromophore combinations containing four different luminescent compounds, *i.e.* anthracene, **23**, **24** and rhodamine 6G (Fig. 17). Photoluminescence studies indicate that the energy transfer process is prevented when one of the chromophores is removed from the assembly.

The co-assembled gel of the peptide amphiphile **25** and the related fluorescent peptide amphiphile **26** (Fig. 18) enables control of the luminescence of chromophores at the periphery of nanofibers.[73] The fluorescence intensity of the co-assembled gels can be tuned through energy transfer to acceptors such as fluorescein, which is tagged to bioactive polysaccharide heparin and incorporated into the gel nanofibers. Evidence for energy transfer was obtained by confocal microscopy from photobleaching of the acceptor (Fig. 18). When a small area of the fibers is saturated with light, photobleaching of the acceptor occurs, which is accompanied by immediate recovery of the donor fluorescence. This strategy could be useful for investigating the interaction of soft materials with proteins.

Xue, Lu *et al.* reported the amplification of emission enhancement in a gel formed by mixing **27** and **28** (Fig. 19), which have similar structures and are characterized by fluorescence quantum efficiencies of 0.02 and 0.15, respectively, in DMSO.[74] Molecule **27** alone shows a weak enhancement of emission upon

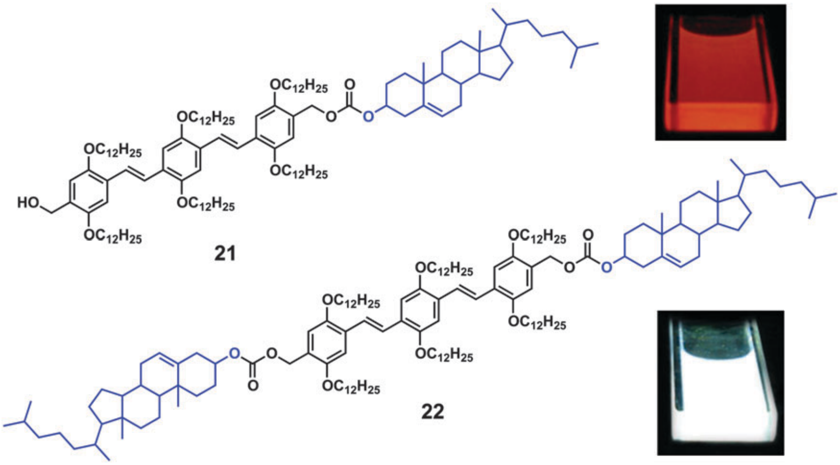

Fig. 16 Molecular structures of cholesterol appended OPV gelators. Insets show the red-light and white-light emission of the related gels under illumination at 365 nm, in the presence of acceptor **20**. (Adapted with permission from ref. 66. Copyright 2009 Wiley-VCH.)

This journal is © The Royal Society of Chemistry 2014

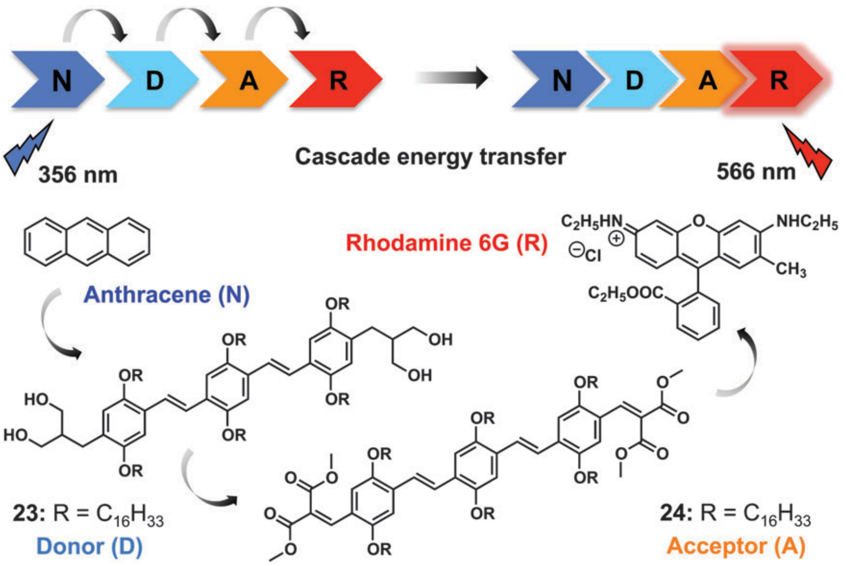

Fig. 17 Molecular structures of the four components of a gel mixture affording a cascade of photoinduced energy transfer processes. (Adapted with permission from ref. 72. Copyright 2012 Wiley-VCH.)

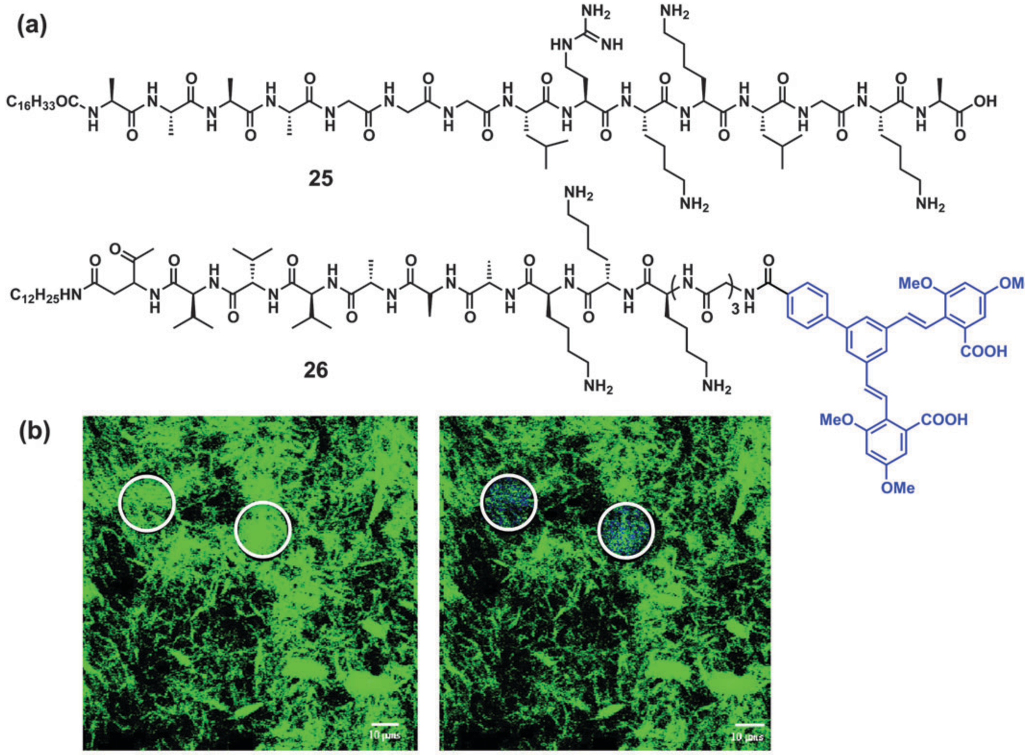

Fig. 18 (a) Molecular structures of peptide amphiphiles **25** and **26**. (b) Confocal microscopy images of bundles of **25**/**26** co-assemblies before (left) and after photobleaching (right). When the area in the white circle is bleached, a recovery of the donor emission is observed. The blue areas correspond to emission from **26** (donor) whereas green areas are due to emission of fluorescein (acceptor) attached to heparin. (Adapted with permission from ref. 73. Copyright 2007 American Chemical Society.)

gelation in a 4 : 1 DMSO–H_2O solution due to H-aggregation. A two-component gel prepared by the addition of **28** (1.6 mol%) to **27** in DMSO–H_2O shows a 23-fold fluorescence intensity enhancement in comparison to the corresponding solution. The emission intensity enhancement promoted by excitation energy transfer is facilitated by the strong spectral overlap between the donor emission and acceptor absorption, as well as the ability of the components to cooperatively aggregate and induce co-assembly. As the fluorescence of **28** is sensitive to protons, the proton response of the two-component gels was also

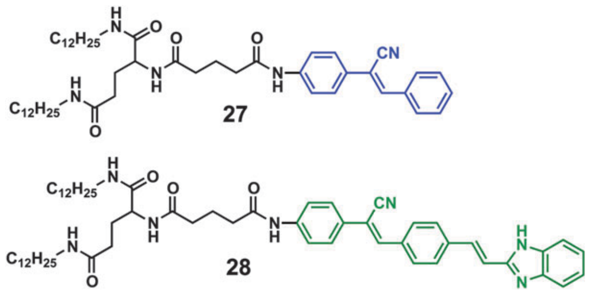

Fig. 19 Molecular structures of an energy transfer donor (**27**) and acceptor (**28**).

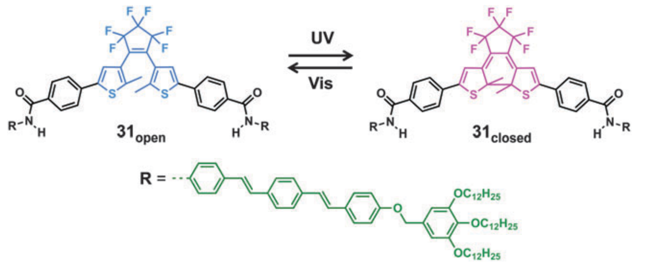

Fig. 21 Molecular structure of the OPV-equipped diarylethene **31** in its open and closed form.

successfully tested in order to explore the possibility that wet gels may serve as fluorescent sensory materials for volatile acids.

Rao, George and coworkers demonstrated a supramolecular co-facial assembly of the OPV donor **29** and the PBI acceptor **30** in water, which form hydrogels with remarkable elastic and conducting properties (Fig. 20).[75,76] In water, the T-shaped OPV **29** forms noncovalent amphiphilic pairs with **30** through synergistic π–π stacking, charge-transfer (CT) and electrostatic interactions, which cooperatively contribute to form one-dimensional self-assembled nanostructures (Fig. 20b). Detailed studies show the formation of CT nanotubes by the co-facial organisation of OPV and PBI chromophores with high conductivity properties. Interestingly, titration of **29** with increasing amounts of **30** leads to non-linear fluorescence quenching by exciting at 380 nm. This is attributed to energy transfer from **29** to the non-fluorescent mixed CT-pairs incorporated in the self-assembled nanostructures, which act as energy traps (Fig. 20c).

Recently, Yagai *et al.*, reported the photoresponsive self-aggregation behavior of a diarylethene (DAE) derivative containing OPVs, which undergoes reversible ring-closing and ring-opening reactions by irradiation with UV and visible light, respectively (Fig. 21).[77] The aggregation properties of the open and closed forms are studied in detail and a higher aggregation ability is observed in the flexible open form when compared to the rigid closed form. This observation suggests that the two methyl groups of the DAE core can regulate the aggregation of the open form $\mathbf{31}_{open}$ by a strong π–π stacking interaction between the two π-conjugated wings. Furthermore, the closed isomer $\mathbf{31}_{closed}$, undergoes fluorescence quenching of the π-conjugated wings in nonpolar media, owing to energy transfer within the aggregates and intramolecular energy transfer from the π-conjugated moieties to the DAE core.

6. Energy transfer in self-assembled di- and triblock systems

Rod-coil type block copolymers containing electronically active π-conjugated molecules as a rigid motif can self-organise and form architectures of different sizes and shapes.[78,79] The incorporation of suitable donor–acceptor molecules to such systems may provide functional supramolecular architectures that undergo energy transfer processes taking advantage of the characteristic microphase segregating properties of the diblock polymers.

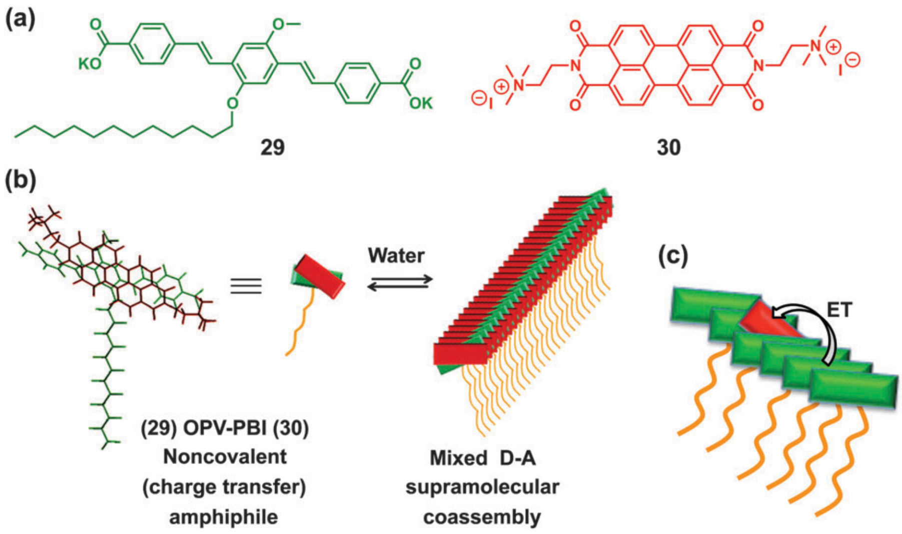

Fig. 20 (a) Molecular structures of the amphiphilic OPV **29** and of PBI **30**. Schematic representation of (b) a noncovalent **29**/**30** charge-transfer amphiphile and its self-assembly into 1-D supramolecular structures and (c) energy transfer from **29** to the non-fluorescent mixed CT-pairs incorporated into the self-assembled nanostructures. (Adapted with permission from ref. 75. Copyright 2012 Wiley-VCH.)

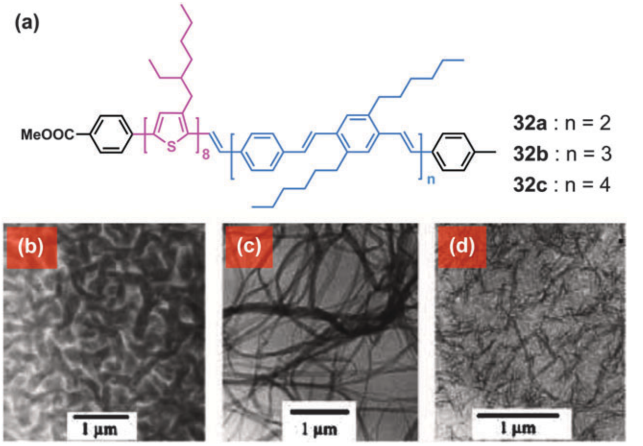

Fig. 22 (a) Molecular structures of rod–rod diblock polymers containing thiophene and OPV. Transmission electron microscopy (TEM) images of the films of the copolymers show different morphologies depending on the composition of the OPV block; (b) **32a**, interwoven network, (c) **32b**, layered stripes and (d) **32c**, lamellae. (Adapted with permission from ref. 80. Copyright 2002 Wiley-VCH.)

Extensive studies on rod–coil type diblock systems have been reported, but rod–rod conjugated diblock systems are much less explored. An interesting example in this category was reported by Yu and co-workers.[80] They synthesized a few rod–rod type co-oligomers consisting of liquid crystalline phenylenevinylene and thiophene blocks, **32a–c** (Fig. 22). Morphological studies show that the composition of the diblock copolymers significantly affects the structure of the resulting self-assembly (Fig. 22). Steady-state luminescence studies demonstrate that excitation of the OPV segments results in strong emission from the thiophene units. Excitation and time-resolved spectroscopy unambiguously prove the occurrence of intramolecular OPV → oligo(thiophene) energy transfer.

The donor–bridge–acceptor system **33** reported by Janssen and coworkers, provides an excellent example of supramolecularly controlled photoinduced energy and electron transfer (Fig. 23).[81] For this purpose, an OPV donor and a PBI acceptor are attached to opposite ends of a long foldable *m*-phenyleneethynylene oligomer. In good solvents the oligomer bridge adopts a random coil conformation in which the interaction between the donor and acceptor chromophores is small. Upon photoexcitation, only long-range intramolecular energy transfer occurs. After the addition of a poor solvent, the *m*-phenyleneethynylene bridge adopts a folded conformation in which the donor and acceptor are closer and undergo electron transfer under light irradiation.

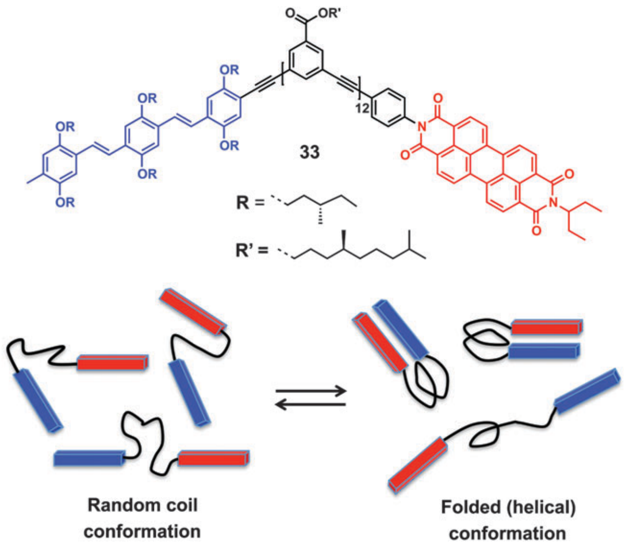

Fig. 23 Top: molecular structure of foldable donor–bridge–acceptor system **33**. Bottom: schematic representation of the different conformational states of **33**. (Adapted with permission from ref. 81. Copyright 2004 American Chemical Society.)

7. Energy transfer in self-assembled OPV nanoparticles

Energy transfer studies in OPV nanoparticles doped with oligomers having relatively long conjugation lengths were successfully demonstrated by Oelkrug, Hanack and co-workers (Fig. 24).[82,83] The doped OPV nanoparticles were prepared by co-precipitation of **34** (host) and **35** (guest) in mixed methanol–water solutions and were characterized by dynamic light scattering (diameter 20–200 nm). The close intermolecular contacts and parallel orientation of **34** in the nanoparticles make them suitable for excitation energy transfer to partners emitting at

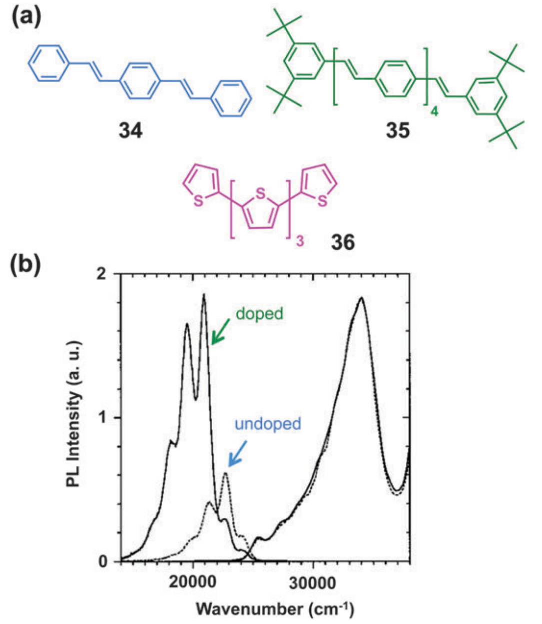

Fig. 24 (a) Molecular structures of the energy transfer donor **34** and acceptors **35** and **36**. (b) Emission and excitation spectra of nanoparticle suspensions of **34**: undoped (dashed lines, excitation spectrum recorded for fluorescence at 22 000 $\mathrm{cm^{-1}}$) and doped with **35** (solid lines, excitation spectrum recorded for fluorescence at 17 500 $\mathrm{cm^{-1}}$). (Adapted with permission from ref. 82. Copyright 1998 American Chemical Society.)

lower energies (*i.e.* OPVs having higher conjugation lengths). Excitation of **34** in the presence of small amounts of dopant **35** shows the typical fluorescence of the latter. Additionally, the excitation spectrum of the guest molecule is found to be identical to the absorption spectrum of **34.** These observations indicate the efficient energy transfer from the host to the entrapped guest molecules (Fig. 24). Similar results were obtained when the oligo(thiophene) derivative **36** was used as the energy trap.[84] Steady state emission and anisotropy studies show that the nanoparticle matrix of **34** provides an anisotropic and highly ordered environment for **36.** The parallel alignment of guest molecules with the host preserves a high degree of fluorescence polarization during the host → guest energy transfer.

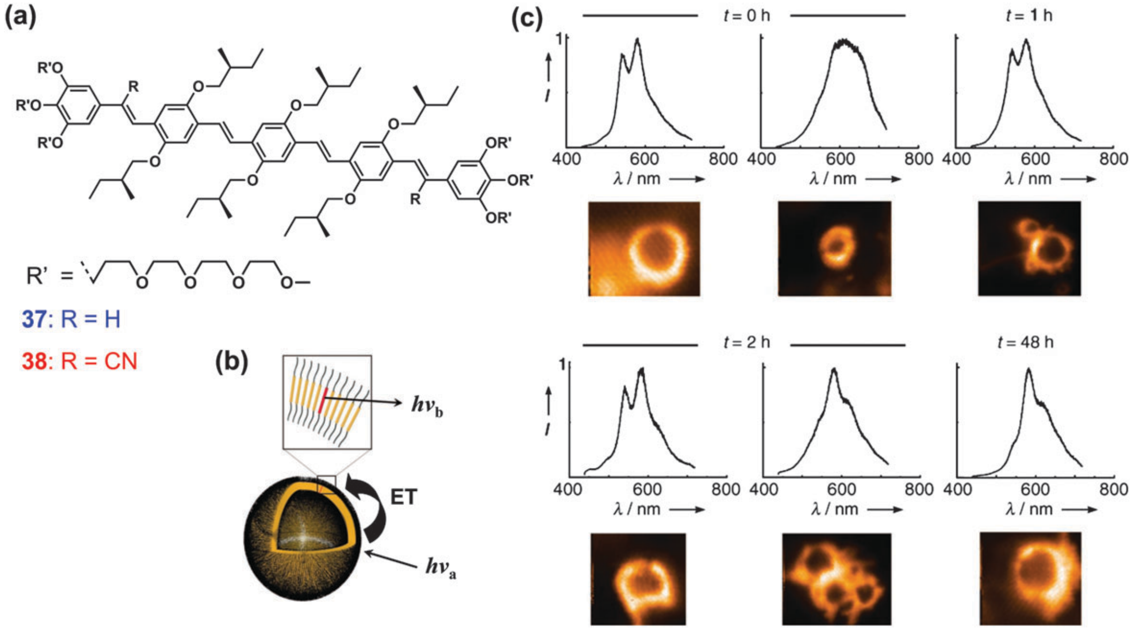

Fig. 25 (a) Molecular structures of amphiphilic OPV-based energy transfer donor **37** and acceptor **38**. (b) Schematic representation of the vesicular self-assembly. (c) Scanning confocal microscopy images and normalized fluorescence (λ_{exc} = 411 nm) of single vesicles showing the morphological transition upon prolonged heating of a 2 mol% solution of **38** at 35 °C. At *t* = 0 h and *t* = 1 h, vesicles of **37** and some vesicles of **38** predominate. At *t* = 2 h, energy transfer starts to appear. After 48 h, all of the vesicles are mixed and show luminescence from the acceptor OPV. (Adapted with permission from ref. 85. Copyright 2006 Wiley-VCH.)

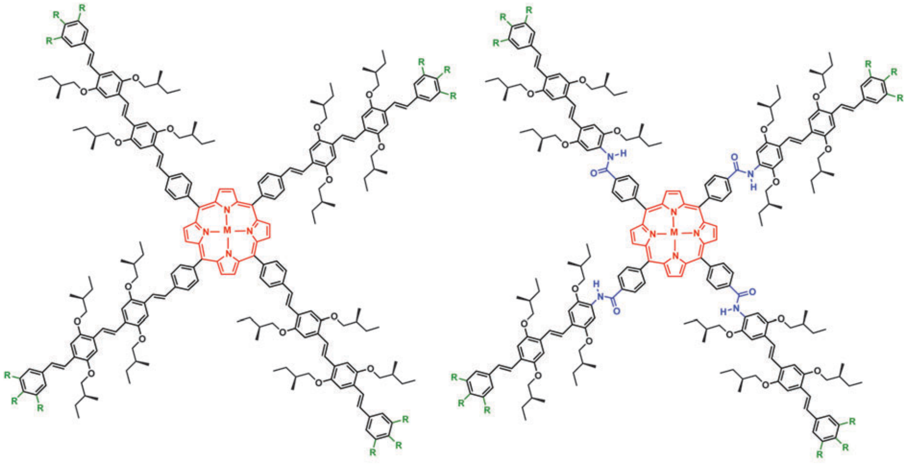

39: R = $(OCH_2CH_2)_4CH_3$; M = 2H
40: R = $(OCH_2CH_2)_4CH_3$; M = Zn
41: R = $OC_{12}H_{25}$; M = 2H
42: R = $OC_{12}H_{25}$; M = Zn

43: R = $OC_{12}H_{25}$; M = 2H
44: R = $OC_{12}H_{25}$; M = Zn

Fig. 26 Molecular structures of hydrophilic (**39**, **40**) and lipophilic (**41–44**) OPV–porphyrin systems.

8. Energy transfer in amphiphilic OPV self-assemblies

Energy and electron transfer studies of organised self-assemblies of π-conjugated systems in aqueous media are a challenging task due their high hydrophobicity. To overcome this problem, Schenning, Meijer and co-workers rationally designed the amphiphilic OPVs **37** and **38** (Fig. 25).[85] In an aqueous environment, these OPV molecules form self-assembled vesicular structures as determined by dynamic light scattering and scanning confocal microscopy. Since the cyano-substituted derivative **38** has a lower optical band gap than the parent derivative **37**, it serves as an energy acceptor upon co-assembling in a vesicular structure. The energy transfer processes were studied at the single vesicle level, by visualizing individual and mixed vesicular assemblies, using scanning confocal microscopy (Fig. 25c).

Sequential energy and electron transfer in mixed π-conjugated assemblies have been demonstrated by the OPV–porphyrin systems **39** and **40** in water (Fig. 26).[86,87] The strong hydrophobicity of the π-conjugated moieties forces them to form H-type aggregates in water to minimize contact with the polar environment. Selective excitation of the OPV units results in the stepwise transfer of excitation energy to the zinc and then to the free-base porphyrin. Moreover, incorporation of C_{60} into mixed aggregates of **39** and **40** affords an additional electron transfer step to C_{60}. The lipophilic analogues **41** and **42** (Fig. 26) were prepared by changing the ethylene oxide chains to alkyl chains.[86] Interestingly, these derivatives form J-type aggregates in organic solvents, as inferred by their optical properties. They also show the stepwise energy transfer observed in the previous case and the efficiency is found to be higher for the couple **42**/**41** than for **40**/**39**.

The effect of the supramolecular organization of π-stacked assemblies on energy transfer was proved by comparing the properties of the donor–acceptor system **44**/**43** (Fig. 26) with that of **40**/**39** and **42**/**41**.[87] Optical studies suggest that the presence of intermolecular hydrogen bonding substantially improves the organisation of the chromophores in the self-assembled state, which consequently enhances the efficiency of energy transfer in the co-assembled state. In all of the systems studied, the difference in the efficiency of energy transfer is correlated to the specific chromophore organisation within the co-assemblies.

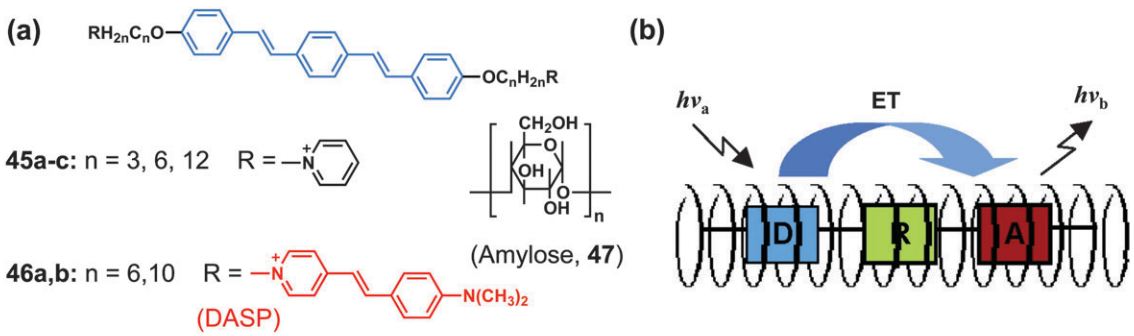

Fig. 27 (a) Molecular structures of amphiphilic OPVs functionalised with energy acceptors (**45** and **46**) and amylose (**47**). (b) Schematic representation of the directional energy transfer process in amylose encapsulated A–OPV–A chromophores. (Adapted with permission from ref. 88. Copyright 2006 American Chemical Society.)

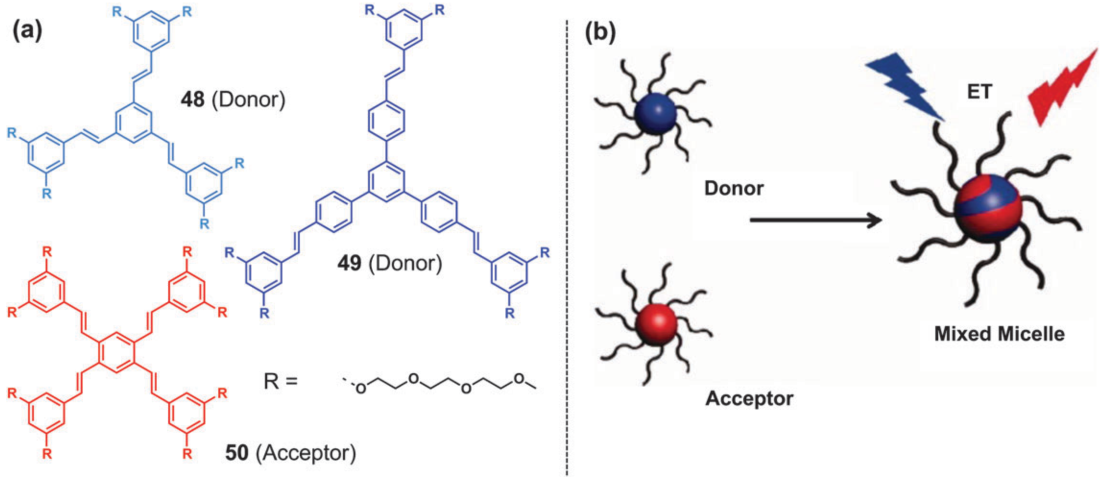

Fig. 28 (a) Molecular structures of amphiphilic conjugated dendrimers **48**, **49**, and **50**. (b) Schematic representation of the formation of mixed micelles between donor and acceptor units. (Adapted with permission from ref. 90. Copyright 2013 Wiley-VCH.)

Kim and co-workers reported efficient energy transfer in acceptor–donor–acceptor (A–D–A) linear chain chromophores based on amphiphilic OPV donors in combination with several energy acceptors (**45** and **46**, Fig. 27) encapsulated within the helical structures of amylose (**47**, Fig. 27).[88,89] Photoinduced processes in the presence and absence of the helical encapsulation show that efficiency depends upon the D–A distance and nature of the acceptor. For example, excitation of the helically encapsulated **46b** at 375 nm in water leads to over 99% quenching of the OPV fluorescence when compared to the weak acceptor **45c** (λ_{em} = 432 nm). Energy transfer from OPV to the *N*,*N*-dimethylaminostyryl-4-pyridinium (DASP) unit brings about a 10-fold increase in the acceptor fluorescence intensity when compared to the selective excitation of the acceptor at 480 nm. In the absence of amylose, excitation of either OPV or DASP showed no measurable difference in emission intensity, which highlights the importance of helical encapsulation in the observed energy transfer process.

An efficient energy transfer process between the amphiphilic conjugated dendrimers **48**, **49** (donors) and acceptor **50**, with OPV cores and oligo(ethylene oxide) termini forming micellar structures in water was presented by Dai, Baek and co-workers (Fig. 28).[90] The formation of donor–acceptor aggregates enable an efficient energy transfer, which strongly depends on the distance of the involved partners. Also the effect of co-solvent, temperature and concentration is studied, allowing a deeper understanding of the photophysical properties of the micelles.

9. Energy transfer in hybrids made of OPVs and inorganic materials

Stupp and co-workers demonstrated energy transfer in nanostructured OPV–silicate hybrid films, loaded with rhodamine B (Fig. 29).[91] The hydrophilic segment of the amphiphilic OPV molecules **50a–d** interacts with precursors of silica and self-assembles into an ordered phase during solvent evaporation. Morphological and spectroscopic studies of OPV–silicate films show that a thin layer of silicate separates OPV domains in the hybrid film. In order to study how the morphology of the hybrid films affects the efficiency of energy transfer, a rhodamine B derivative (**51**) was covalently grafted to the inorganic portion of the **51a**–silicate film. Comparison between the amorphous **51a**–poly(2-hydroxyethyl methacrylate) film with the **50a**–silicate material shows a better efficiency in the latter case. Fig. 29c shows a photograph of the **50a**–polymer film and **50a**–silicate film in the presence of 2 mol% of the acceptor, which shows red fluorescence of rhodamine B from the silicate film only. This is attributed to the shorter distance between donors and acceptors and also to efficient energy migration within the organic domains of this specific film.

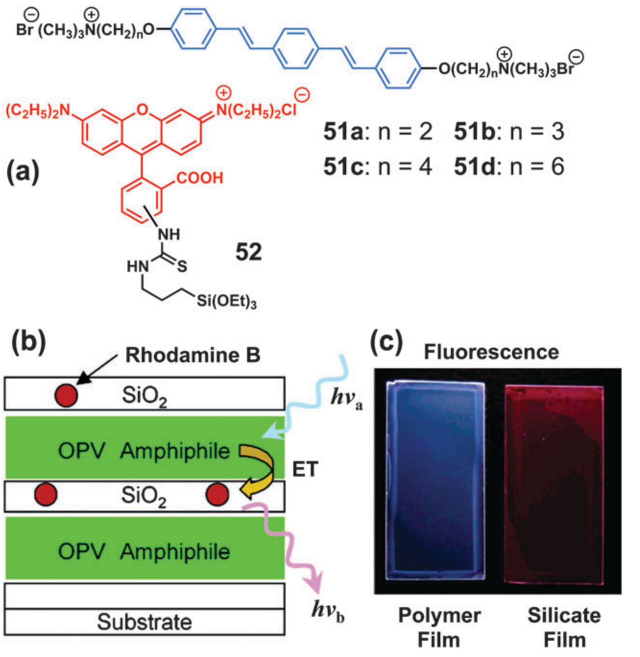

Fig. 29 (a) Molecular structures of OPV amphiphiles (**51a–d**) and of the rhodamine B derivative (**52**) used to prepare hybrid silicate films. (b) Schematic representation of the energy transfer process in **51a**–silicate hybrid films when doped with **52**. (c) Photographs under UV irradiation (λ_{ex} = 365 nm) of a **51a**–poly(2-hydroxyethyl methacrylate) film (left) and a **51a**–silicate film (right), obtained from precursor solutions containing 2 mol% of **52**. (Adapted with permission from ref. 91. Copyright 2006 American Chemical Society.)

Inagaki *et al.* described the efficient visible light emission of rubrene-doped mesostructured OPV functionalised organosilica. This material was prepared using a triethoxysilane functionalised OPV (**53**), and tetraethyl orthosilicate (TEOS), in the presence of templating surfactant **54** (Fig. 30a).[92] The dopant rubrene was dispersed in the mesochannels of the fluorescent OPV–silica framework, thereby facilitating the formation of light harvesting donor–acceptor pairs (Fig. 30b). Colour tuning of the emission of the rubrene doped OPV–silica films from blue to yellow was obtained by mixing the colour of

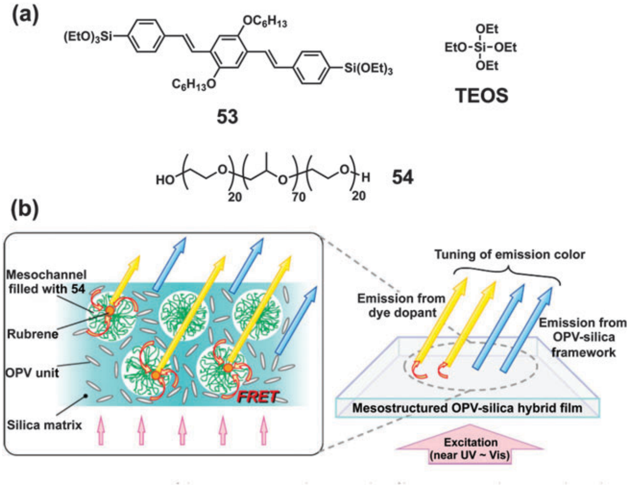

Fig. 30 (a) Molecular structures of the components used for the preparation of fluorescent mesostructured organosilica films. (b) Schematic illustration of the energy transfer process in the rubrene doped OPV–silica hybrid film. (Adapted with permission from ref. 92. Copyright 2009 Wiley-VCH.)

the two luminophores as a function of doping. The enhancement of the emission output by increasing the amount of the rubrene acceptor confirms a non-radiative energy transfer process and not a trivial re-absorption of the emitted light by the OPV–silica framework.

Energy transfer within a hybrid soft material consisting of gold nanoparticles and self-assembled OPV nanotapes has been recently reported.[93] The OPV derivative **55** that forms a gel in toluene was selected as a template, whereas another OPV derivative (**56**) containing a disulfide moiety at one end was used to bind gold nanoparticles (Fig. 31). Co-assembled hybrid gels were prepared by mixing **55** and **56**–Au in toluene at different ratios, followed by heating and cooling. Formation of supramolecular hybrid nanotapes is confirmed by cryo-TEM, which shows arrays of gold particles on both sides of the tape. Incorporation of **56**–Au into the tapes caused quenching of the photoluminescence (Fig. 31) as well as shortening of the lifetime of **55**, due to the transfer of electronic excitation from OPVs to the docked gold nanoparticles. Further confirmation of energy transfer is obtained from photoinduced absorption studies, which show a clear difference in the population of the lowest electronic excited states of **55** and **55**/**56**–Au hybrid gels in the nanosecond time scale.

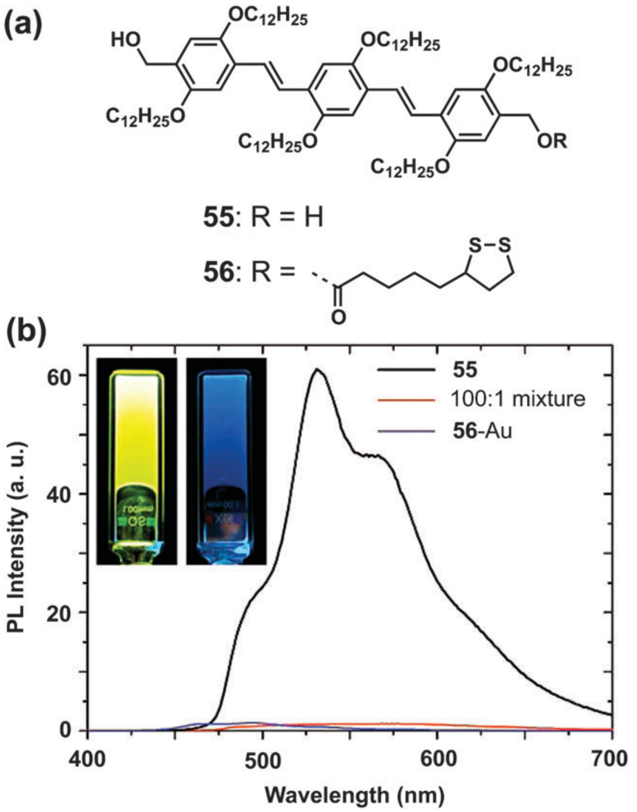

Fig. 31 (a) Molecular structures of the OPV gelator **55** and of the disulfide functionalised analogue **56**. (b) Fluorescence spectrum of a 100 : 1 mixed gel of **55** and **56**–Au and of the individual compounds in toluene. Inset: photographs of the luminescent gel **55** (left) and of the 100 : 1 **55**/**56**–Au mixed gel (right). The latter displays a faint blue emission that can be ascribed to individual **55** molecules. (Adapted with permission from ref. 93. Copyright 2007 Wiley-VCH.)

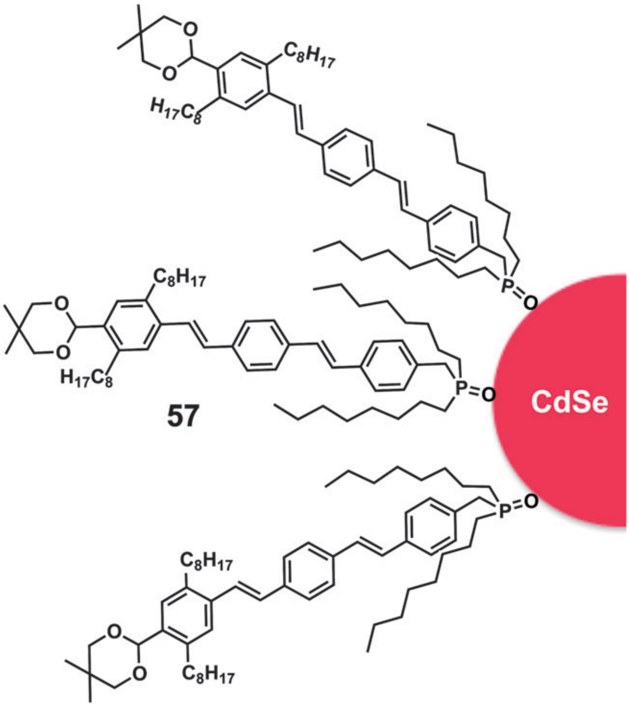

Fig. 32 Schematic representation of a CdSe quantum dot covered with the OPV ligand **57** (Adapted with permission from ref. 95. Copyright 2008 American Chemical Society.)

The drawback of polydispersity of chain lengths in π-conjugated systems anchored to CdSe quantum dots (QDs) in 'grafting-from' polymerization[94] was overcome by synthesizing the OPV ligand **57** and attaching it to QDs through a 'grafting-to' (*i.e.* ligand exchange) method (Fig. 32).[95,96] The solid state emission spectrum of thin films of CdSe QDs covered with **57** shows primarily the features of the QDs, as a result of an efficient OPV → QD energy transfer. The excitation spectrum of **57**–CdSe, recorded by collecting the emission of QDs, matches the absorption spectrum of OPV and confirms the energy transfer process. Interestingly, the **57** functionalised CdSe QDs display a one-dimensional emission dipole moment in contrast to the two-dimensional degenerate dipole moments typically observed for QDs.

Schenning, Meskers and co-workers studied the photophysical behavior of OPV-functionalised gold nanoparticles (**58**, Fig. 33), observing a considerable quenching of the highly emissive OPV molecule upon photoexcitation.[97] The fluorescence and photoinduced absorption spectroscopy show that the emission quenching and the shortening of the lifetime of OPV are due to ultrafast resonance energy transfer to the gold nanoparticles, rather than electron transfer.

The synthesis and energy transfer studies of hybrid materials containing a coordination compound (Cu(I)–bisphenanthroline) and OPV moieties have been also reported (Fig. 34).[98,99] These multicomponent systems **59a,b** show efficient intramolecular energy transfer from the lowest singlet excited state of the OPV arms to the Cu(I)-complexed core. Notably, the nature of the photoinduced processes is found to be dependent

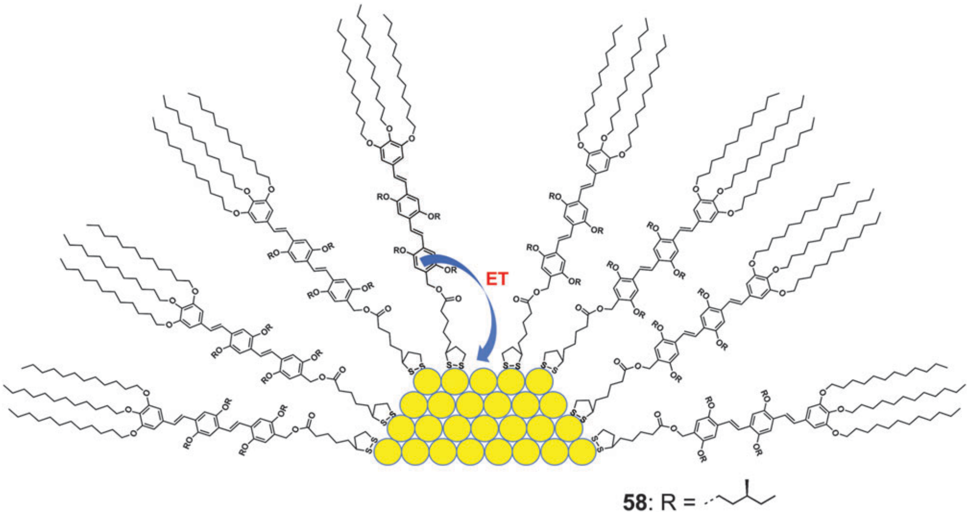

Fig. 33 Schematic representation of OPV functionalised gold nanoparticles **58**. (Adapted with permission from ref. 97. Copyright 2007 Elsevier Ltd)

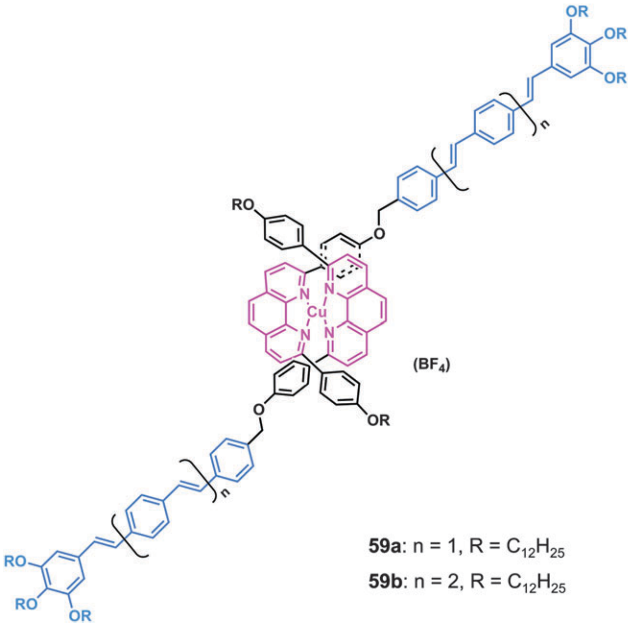

Fig. 34 Molecular structures of Cu(I)–bisphenanthroline complexes with appended OPV units.

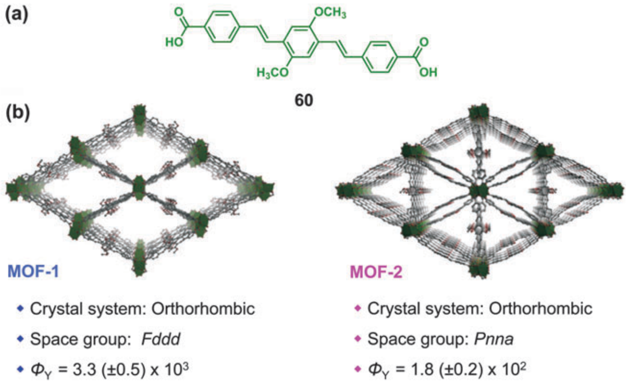

Fig. 35 (a) Molecular structure of the OPV ligand **60** and (b) projection of the MOFs viewed along the *a* crystallographic direction. (Adapted with permission from ref. 100. Copyright 2009 The Royal Society of Chemistry.)

on the length of the conjugated OPV backbone. In the complex **59a**, equipped with a trimeric OPV fragment, irradiation of OPV results in quantitative sensitisation of the Cu(I) complex. This is not observed for **59b**, suggesting that electron transfer may play a role when longer OPV fragments are present. Indeed, the different behavior of **59b** is ascribed to the slightly increased electron-accepting character of the OPV tetrameric unit when compared to the corresponding trimer.

Petoud, Rosi and co-workers reported the synthesis and characterization of NIR emitting metal–organic frameworks (MOFs) based on carboxylic acid functionalised OPV **60** and ytterbium cations (Fig. 35).[100] Photoluminescence studies revealed that the OPV ligand can sensitize the Yb^{3+} NIR emission through energy transfer (antenna effect). Interestingly, the luminescence quantum yields of MOFs (Fig. 35b) were found to be among the highest ever reported for ytterbium systems in solution. This indicates that the rigid extended structure of the MOFs provides protection for the lanthanide cations from solvent vibrations, affording remarkable NIR photoluminescent materials.

10. Conclusion

OPVs are one of the most extensively investigated classes of linear π-systems. The optical and electronic properties of these molecules are strongly dependent on the extent of conjugation, the specific substituents chosen and also on intermolecular interactions, primarily driven by non-covalent stacking. Supramolecular architectures of different sizes and shapes can be created with the help of hydrogen bonding and π-interactions. The photophysical properties of the resulting materials are substantially different when compared to those of the constituent molecules. In particular, self-assembled OPV aggregates and gels have turned out to be excellent scaffolds for hosting suitable excitation energy acceptors, which enable an efficient energy transfer thanks to supramolecular organization. Concentration, polarity of the solvent and temperature changes further allow the tuning of molecular self-assembly as well as the control of energy transfer, leading to emission colour tuning of the material.

We have shown here that a significant amount of knowledge has been generated over the years in the field of OPV-based photoactive supramolecular nanomaterials featuring photoinduced energy transfer. However, much work still needs to be done in order to use this knowledge for practical application. We anticipate that remarkable opportunities exist in the field of photoactive materials based on OPVs and, more generally, on organic conjugated systems, particularly in the context of optoelectronic technologies based on organic nanomaterials that are expected to ultimately be implemented in the years to come.

Acknowledgements

We acknowledge the European Commission for supporting V. K. P. (Marie Curie International Incoming Fellowship, GELBRID; PIIF-GA-2010-276574) at CNR-ISOF. This work was supported by the Italian Ministry of Research (PRIN 2010 INFOCHEM – contract no. CX2TLM; FIRB Futuro in Ricerca SUPRACARBON – contract no. RBFR10DAK6) and Consiglio Nazionale delle Ricerche (SOLARFUELTANDEM project of the 10-EuroSolarFuels-FP-006 EUROCORES Programme of the European Science Foundation; Progetto Bandiera N-CHEM). A. A. is grateful to the Department of Atomic Energy, Government of India for a DAE-SRC Outstanding Researcher Award and CSIR, Government of India for partial financial support under TAPSUN.

References

1 D. Gust, T. A. Moore and A. L. Moore, *Acc. Chem. Res.*, 2001, **34**, 40–48.
2 R. Ballardini, A. Credi, M. Teresa Gandolfi, F. Marchioni, S. Silvi and M. Venturi, *Photochem. Photobiol. Sci.*, 2007, **6**, 345–356.
3 A. C. Benniston and A. Harriman, *Mater. Today*, 2008, **11**, 26–34.
4 G. Calzaferri and K. Lutkouskaya, *Photochem. Photobiol. Sci.*, 2008, **7**, 879–910.
5 A. Ajayaghosh, V. K. Praveen and C. Vijayakumar, *Chem. Soc. Rev.*, 2008, **37**, 109–122.
6 F. Laquai, Y.-S. Park, J.-J. Kim and T. Basché, *Macromol. Rapid Commun.*, 2009, **30**, 1203–1231.
7 V. Balzani, G. Bergamini, P. Ceroni and E. Marchi, *New J. Chem.*, 2011, **35**, 1944–1954.
8 A. Barbieri, B. Ventura and R. Ziessel, *Coord. Chem. Rev.*, 2012, **256**, 1732–1741.
9 K. V. Rao, K. K. R. Datta, M. Eswaramoorthy and S. J. George, *Chem.–Eur. J.*, 2012, **18**, 2184–2194.
10 P. D. Frischmann, K. Mahata and F. Würthner, *Chem. Soc. Rev.*, 2013, **42**, 1847–1870.
11 K. V. Rao, A. Jain and S. J. George, *J. Mater. Chem. C*, 2014, DOI: 10.1039/c3tc31729c.
12 R. E. Martin and F. Diederich, *Angew. Chem., Int. Ed.*, 1999, **38**, 1350–1377.
13 J. Gierschner, J. Cornil and H.-J. Egelhaaf, *Adv. Mater.*, 2007, **19**, 173–191.
14 A. Ajayaghosh and V. K. Praveen, *Acc. Chem. Res.*, 2007, **40**, 644–656.
15 B.-K. An, J. Gierschner and S. Y. Park, *Acc. Chem. Res.*, 2012, **45**, 544–554.
16 J. Gierschner, *Phys. Chem. Chem. Phys.*, 2012, **14**, 13146–13153.
17 J. Gierschner, L. Lüer, B. Milián-Medina, D. Oelkrug and H.-J. Egelhaaf, *J. Phys. Chem. Lett.*, 2013, **4**, 2686–2697.
18 A. P. H. J. Schenning and E. W. Meijer, *Chem. Commun.*, 2005, 3245–3258.
19 E. Moulin, J. J. Cid and N. Giuseppone, *Adv. Mater.*, 2013, **25**, 477–487.
20 N. J. Turro, *Modern Molecular Photochemistry*, University Science Books, Sausalito, 1991.
21 G. D. Scholes, G. R. Fleming, A. Olaya-Castro and R. van Grondelle, *Nat. Chem.*, 2011, **3**, 763–774.
22 J. Strümpfer, M. Şener and K. Schulten, *J. Phys. Chem. Lett.*, 2012, **3**, 536–542.
23 N. Armaroli, F. Barigelletti, P. Ceroni, J.-F. Eckert, J.-F. Nicoud and J.-F. Nierengarten, *Chem. Commun.*, 2000, 599–600.
24 A. Gégout, J. L. Delgado, J.-F. Nierengarten, B. Delavaux-Nicot, A. Listorti, C. Chiorboli, A. Belbakra and N. Armaroli, *New J. Chem.*, 2009, **33**, 2174–2182.
25 J. L. Segura, N. Martín and D. M. Guldi, *Chem. Soc. Rev.*, 2005, **34**, 31–47.
26 T. M. Figueira-Duarte, A. Gégout and J.-F. Nierengarten, *Chem. Commun.*, 2007, 109–119.
27 G. Accorsi and N. Armaroli, *J. Phys. Chem. C*, 2010, **114**, 1385–1403.
28 N. Armaroli, G. Accorsi, J.-P. Gisselbrecht, M. Gross, V. Krasnikov, D. Tsamouras, G. Hadziioannou, M. J. Gómez-Escalonilla, F. Langa, J.-F. Eckert and J.-F. Nierengarten, *J. Mater. Chem.*, 2002, **12**, 2077–2087.
29 N. Armaroli, G. Accorsi, J. N. Clifford, J.-F. Eckert and J.-F. Nierengarten, *Chem.–Asian J.*, 2006, **1**, 564–574.
30 N. Armaroli, *Photochem. Photobiol. Sci.*, 2003, **2**, 73–87.
31 N. Armaroli, J.-F. Eckert and J.-F. Nierengarten, *Chem. Commun.*, 2000, 2105–2106.
32 G. Accorsi, A. Listorti, K. Yoosaf and N. Armaroli, *Chem. Soc. Rev.*, 2009, **38**, 1690–1700.
33 A. P. H. J. Schenning, E. Peeters and E. W. Meijer, *J. Am. Chem. Soc.*, 2000, **122**, 4489–4495.
34 M. Kimura, H. Narikawa, K. Ohta, K. Hanabusa, H. Shirai and N. Kobayashi, *Chem. Mater.*, 2002, **14**, 2711–2717.

35 Akai, H. Nakao, K. Kanemoto, T. Karasawa, H. Hashimoto and M. Kimura, *J. Lumin.*, 2005, **112**, 449–453. Q5

36 Akai, A. Okada, K. Kanemoto, T. Karasawa, H. Hashimoto and M. Kimura, *J. Lumin.*, 2006, **119–120**, 283–287.

37 S. R. Amrutha and M. Jayakannan, *J. Phys. Chem. B*, 2008, **112**, 1119–1129.

38 S. K. Nisha and S. K. Asha, *J. Polym. Sci., Part A: Polym. Chem.*, 2012, **51**, 509–524.

39 S. K. Nisha and S. K. Asha, *J. Phys. Chem. B*, 2013, **117**, 13710–13722.

40 S. S. Babu, J. Aimi, H. Ozawa, N. Shirahata, A. Saeki, S. Seki, A. Ajayaghosh, H. Möhwald and T. Nakanishi, *Angew. Chem., Int. Ed.*, 2012, **51**, 3391–3395.

41 D. K. Maiti and A. Banerjee, *Chem. Commun.*, 2013, **49**, 6909–6911.

42 M. D. Ward, *Chem. Soc. Rev.*, 1997, **26**, 365–375.

43 S. Yagai, *J. Photochem. Photobiol., C*, 2006, **7**, 164–182.

44 D. González-Rodríguez and A. P. H. J. Schenning, *Chem. Mater.*, 2011, **23**, 310–325.

45 E. H. A. Beckers, P. A. van Hal, A. P. H. J. Schenning, A. El-ghayoury, E. Peeters, M. T. Rispens, J. C. Hummelen, E. W. Meijer and R. A. J. Janssen, *J. Mater. Chem.*, 2002, **12**, 2054–2060.

46 M. T. Rispens, L. Sánchez, E. H. A. Beckers, P. A. van Hal, A. P. H. J. Schenning, A. El-ghayoury, E. Peeters, E. W. Meijer, R. A. J. Janssen and J. C. Hummelen, *Synth. Met.*, 2003, **135–136**, 801–803.

47 E. E. Neuteboom, E. H. Beckers, S. C. Meskers, E. W. Meijer and R. A. Janssen, *Org. Biomol. Chem.*, 2003, **1**, 198–203.

48 E. H. A. Beckers, A. P. H. J. Schenning, P. A. van Hal, A. El-ghayoury, L. Sánchez, J. C. Hummelen, E. W. Meijer and R. A. J. Janssen, *Chem. Commun.*, 2002, 2888–2889.

49 F. J. M. Hoeben, L. M. Herz, C. Daniel, P. Jonkheijm, A. P. H. J. Schenning, C. Silva, S. C. J. Meskers, D. Beljonne, R. T. Phillips, R. H. Friend and E. W. Meijer, *Angew. Chem., Int. Ed.*, 2004, **43**, 1976–1979.

50 C. Daniel, L. M. Herz, D. Beljonne, F. J. M. Hoeben, P. Jonkheijm, A. P. H. J. Schenning, E. W. Meijer, R. T. Phillips and C. Silva, *Synth. Met.*, 2004, **147**, 29–35.

51 D. Beljonne, E. Hennebicq, C. Daniel, L. M. Herz, C. Silva, G. D. Scholes, F. J. M. Hoeben, P. Jonkheijm, A. P. H. J. Schenning, S. C. J. Meskers, R. T. Phillips, R. H. Friend and E. W. Meijer, *J. Phys. Chem. B*, 2005, **109**, 10594–10604.

52 S. Jang, M. Newton and R. Silbey, *Phys. Rev. Lett.*, 2004, **92**, 218301.

53 F. J. M. Hoeben, A. P. H. J. Schenning and E. W. Meijer, *ChemPhysChem*, 2005, **6**, 2337–2342.

54 M. H. Chang, F. J. M. Hoeben, P. Jonkheijm, A. P. H. J. Schenning, E. W. Meijer, C. Silva and L. M. Herz, *Chem. Phys. Lett.*, 2006, **418**, 196–201.

55 C. Daniel, F. Makereel, L. M. Herz, F. J. M. Hoeben, P. Jonkheijm, A. P. H. J. Schenning, E. W. Meijer and C. Silva, *J. Chem. Phys.*, 2008, **129**, 104701.

56 J. Zhang, F. J. M. Hoeben, M. J. Pouderoijen, A. P. H. J. Schenning, E. W. Meijer, F. C. De Schryver and S. De Feyter, *Chem.–Eur. J.*, 2006, **12**, 9046–9055.

57 F. J. M. Hoeben, M. J. Pouderoijen, A. P. H. J. Schenning and E. W. Meijer, *Org. Biomol. Chem.*, 2006, **4**, 4460–4462.

58 S. S. Babu, K. K. Kartha and A. Ajayaghosh, *J. Phys. Chem. Lett.*, 2010, **1**, 3413–3424.

59 L. Maggini and D. Bonifazi, *Chem. Soc. Rev.*, 2012, **41**, 211–241.

60 S. S. Babu, V. K. Praveen and A. Ajayaghosh, *Chem. Rev.*, 2014, DOI: 10.1021/cr400195e.

61 S. J. George and A. Ajayaghosh, *Chem.–Eur. J.*, 2005, **11**, 3217–3227.

62 V. K. Praveen, S. J. George and A. Ajayaghosh, *Macromol. Symp.*, 2006, **241**, 1–8.

63 S. S. Babu, V. K. Praveen and A. Ajayaghosh, *Macromol. Symp.*, 2008, **273**, 25–32.

64 A. Ajayaghosh, V. K. Praveen, S. Srinivasan and R. Varghese, *Adv. Mater.*, 2007, **19**, 411–415.

65 A. Ajayaghosh, V. K. Praveen, C. Vijayakumar and S. J. George, *Angew. Chem., Int. Ed.*, 2007, **46**, 6260–6265.

66 C. Vijayakumar, V. K. Praveen and A. Ajayaghosh, *Adv. Mater.*, 2009, **21**, 2059–2063.

67 C. Vijayakumar, V. K. Praveen, K. K. Kartha and A. Ajayaghosh, *Phys. Chem. Chem. Phys.*, 2011, **13**, 4942–4949.

68 A. Ajayaghosh, S. J. George and V. K. Praveen, *Angew. Chem., Int. Ed.*, 2003, **42**, 332–335.

69 V. K. Praveen, S. J. George, R. Varghese, C. Vijayakumar and A. Ajayaghosh, *J. Am. Chem. Soc.*, 2006, **128**, 7542–7550.

70 A. Ajayaghosh, C. Vijayakumar, V. K. Praveen, S. S. Babu and R. Varghese, *J. Am. Chem. Soc.*, 2006, **128**, 7174–7175.

71 V. K. Praveen, C. Ranjith and N. Armaroli, *Angew. Chem., Int. Ed.*, 2014, DOI: 10.1002/anie.201306787.

72 S. K. Samanta and S. Bhattacharya, *Chem.–Eur. J.*, 2012, **18**, 5875–15885.

73 H. A. Behanna, K. Rajangam and S. I. Stupp, *J. Am. Chem. Soc.*, 2007, **129**, 321–327.

74 P. Xue, R. Lu, P. Zhang, J. Jia, Q. Xu, T. Zhang, M. Takafuji and H. Ihara, *Langmuir*, 2013, **29**, 417–425.

75 K. V. Rao and S. J. George, *Chem.–Eur. J.*, 2012, **18**, 14286–14291.

76 M. Kumar, K. V. Rao and S. J. George, *Phys. Chem. Chem. Phys.*, 2014, DOI: 10.1039/c3cp54190h.

77 S. Yagai, K. Ishiwatari, X. Lin, T. Karatsu, A. Kitamura and S. Uemura, *Chem.–Eur. J.*, 2013, **19**, 6971–6975.

78 M. Lee, B.-K. Cho and W.-C. Zin, *Chem. Rev.*, 2001, **101**, 3869–3892.

79 H.-J. Kim, T. Kim and M. Lee, *Acc. Chem. Res.*, 2011, **44**, 72–82.

80 H. Wang, M.-K. Ng, L. Wang, L. Yu, B. Lin, M. Meron and Y. Xiao, *Chem.–Eur. J.*, 2002, **8**, 3246–3253.

81 A. Marcos Ramos, S. C. J. Meskers, E. H. A. Beckers, R. B. Prince, L. Brunsveld and R. A. J. Janssen, *J. Am. Chem. Soc.*, 2004, **126**, 9630–9644.

82 D. Oelkrug, A. Tompert, J. Gierschner, H.-J. Egelhaaf, M. Hanack, M. Hohloch and E. Steinhuber, *J. Phys. Chem. B*, 1998, **102**, 1902–1907.

This journal is © The Royal Society of Chemistry 2014

83 J. Gierschner, H.-J. Egelhaaf, D. Oelkrug and K. Müllen, *J. Fluoresc.*, 1998, **8**, 37–44.

84 H.-J. Egelhaaf, J. Gierschner and D. Oelkrug, *Synth. Met.*, 2002, **127**, 221–227.

85 F. J. M. Hoeben, I. O. Shklyarevskiy, M. J. Pouderoijen, H. Engelkamp, A. P. H. J. Schenning, P. C. M. Christianen, J. C. Maan and E. W. Meijer, *Angew. Chem., Int. Ed.*, 2006, **45**, 1232–1236.

86 M. Wolffs, F. J. M. Hoeben, E. H. A. Beckers, A. P. H. J. Schenning and E. W. Meijer, *J. Am. Chem. Soc.*, 2005, **127**, 13484–13485.

87 F. J. M. Hoeben, M. Wolffs, J. Zhang, S. De Feyter, P. Leclère, A. P. H. J. Schenning and E. W. Meijer, *J. Am. Chem. Soc.*, 2007, **129**, 9819–9828.

88 O.-K. Kim, J. Je and J. S. Melinger, *J. Am. Chem. Soc.*, 2006, **128**, 4532–4533.

89 J. Je and O.-K. Kim, *Macromol. Symp.*, 2007, **249–250**, 44–49.

90 D. W. Chang, S.-Y. Bae, L. Dai and J.-B. Baek, *J. Polym. Sci., Part A: Polym. Chem.*, 2013, **51**, 168–175.

91 K. Tajima, L.-s. Li and S. I. Stupp, *J. Am. Chem. Soc.*, 2006, **128**, 5488–5495.

92 N. Mizoshita, Y. Goto, T. Tani and S. Inagaki, *Adv. Mater.*, 2009, **21**, 4798–4801.

93 J. van Herrikhuyzen, S. J. George, M. R. J. Vos, N. A. J. M. Sommerdijk, A. Ajayaghosh, S. C. J. Meskers and A. P. H. J. Schenning, *Angew. Chem., Int. Ed.*, 2007, **46**, 1825–1828.

94 N. I. Hammer, T. Emrick and M. D. Barnes, *Nanoscale Res. Lett.*, 2007, **2**, 282–290.

95 P. K. Sudeep, K. T. Early, K. D. McCarthy, M. Y. Odoi, M. D. Barnes and T. Emrick, *J. Am. Chem. Soc.*, 2008, **130**, 2384–2385.

96 P. K. Sudeep and T. Emrick, *ACS Nano*, 2009, **3**, 4105–4109.

97 J. van Herrikhuyzen, R. A. J. Janssen, A. P. H. J. Schenning and S. C. J. Meskers, *Chem. Phys. Lett.*, 2007, **433**, 340–344.

98 N. Armaroli, G. Accorsi, J.-P. Gisselbrecht, M. Gross, J.-F. Eckert and J.-F. Nierengarten, *New J. Chem.*, 2003, **27**, 1470–1478.

99 N. Armaroli, G. Accorsi, Y. Rio, J.-F. Nierengarten, J.-F. Eckert, M. J. Gómez-Escalonilla and F. Langa, *Synth. Met.*, 2004, **147**, 19–28.

100 K. A. White, D. A. Chengelis, M. Zeller, S. J. Geib, J. Szakos, S. Petoud and N. L. Rosi, *Chem. Commun.*, 2009, 4506–4508.